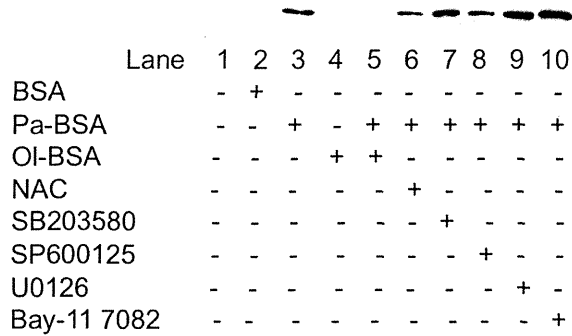


The images in Figures 2C, 3B and 3D are derived from one immunoblot film. The unprocessed, full-length blot is shown below. The addition of this Supplementary Figure will not affect the conclusions of Figures 2 or 3 at all.



**Fig S.** One set of experiments was divided into three parts (Fig. 2C, 3B and 3D) for a better understanding. RAW 264.7 cells were starved for 2 h in serum-free medium, pretreated with NAC, SB203580, SP600125, U0126, or Bay-11 7082 for 1 h, and stimulated with BSA, palmitate/BSA (Pa-BSA), or oleate/BSA (OI-BSA). The histone H3 levels in the supernatants after 16 h were analyzed by western blotting. All the treatments above were performed simultaneously. Lanes 1, 2, 3, and 4 are used in Fig 2C, lanes 1, 2, 3, and 6 are used in Fig 3B, and lanes 1, 2, 3, 7, 8, 9, and 10 are used in Fig 3D.

## Preventive effects of *Morus alba L.* anthocyanins on diabetes in Zucker diabetic fatty rats

ARIYA SARIKAPHUTI<sup>1</sup>, THAMTHIWAT NARARATWANCHAI<sup>1</sup>, TERUTO HASHIGUCHI<sup>2</sup>, TAKASHI ITO<sup>3</sup>, SITA THAWORANUNTA<sup>4</sup>, KIYOSHI KIKUCHI<sup>5</sup>, YOKO OYAMA<sup>2</sup>, IKURO MARUYAMA<sup>3</sup> and SALUNYA TANCHAROEN<sup>6</sup>

<sup>1</sup>School of Anti-Aging and Regenerative Medicine, Mae Fah Luang University, Bangkok 10110, Thailand;

Departments of <sup>2</sup>Laboratory and Vascular Medicine, and <sup>3</sup>Systems Biology in Thromboregulation, Kagoshima University Graduate School of Medical and Dental Sciences, Kagoshima 890-8520, Japan;

<sup>4</sup>Department of Prosthodontics, Faculty of Dentistry, Mahidol University, Bangkok 10400, Thailand;

<sup>5</sup>Departments of Physiology and Neurosurgery, Kurume University School of Medicine, Fukuoka 830-0011, Japan;

<sup>6</sup>Department of Pharmacology, Faculty of Dentistry, Mahidol University, Bangkok 10400, Thailand

Received March 13, 2013; Accepted June 14, 2013

DOI: 10.3892/etm.2013.1203

**Abstract.** The mulberry plant (*Morus alba L.*) contains abundant anthocyanins (ANCs), which are natural antioxidants. The aim of this study was to determine the ANC composition of Thai *Morus alba L.* fruits and to assess the effect of an ANC extract on blood glucose and insulin levels in male leptin receptor-deficient Zucker diabetic fatty (ZDF) rats. The major components of the ANC extract were identified by high-performance liquid chromatography-electrospray ionization-mass spectrometry. ZDF and lean rats were treated with 125 or 250 mg ANCs/kg body weight, or 1% carboxymethylcellulose (CMC) twice daily for 5 weeks. Neither ANC dose had an effect on body weight. Following 5 weeks of treatment, glucose levels were observed to increase from 105.5±8.7 to 396.25±21 mg/dl ( $P<0.0001$ ) in the CMC-treated ZDF rats; however, the glucose levels were significantly lower in the rats treated with 125 or 250 mg/kg ANCs (228.25±45 and 131.75±10 mg/dl, respectively;  $P<0.001$  versus CMC). The administration of 250 mg/kg ANCs normalized glucose levels in the ZDF rats towards those of the lean littermates. Insulin levels were decreased significantly in the ZDF rats treated with CMC or 125 mg/kg ANCs ( $P<0.0001$ ), but not in the rats treated with 250 mg/kg ANCs. Histologically, 250 mg/kg ANCs was observed to prevent islet degeneration compared with the islets in CMC-treated rats. This study, demonstrated that ANCs extracted from *Morus alba L.* were well tolerated

and exhibited effective anti-diabetic properties in ZDF rats. ANCs represent a promising class of therapeutic compounds that may be useful in the prevention of type 2 diabetes.

### Introduction

Type 2 diabetes is preceded by the inability of  $\beta$ -cells to secrete sufficient insulin to overcome insulin resistance or reduced insulin sensitivity, combined with reduced insulin secretion. Degeneration of the islets of Langerhans with  $\beta$ -cell loss is secondary to insulin resistance and is regarded as the pathophysiology of type 2 diabetes (1). Oral hypoglycemic agents directly stimulate insulin release from  $\beta$ -cells to overcome insulin resistance and normalize blood glucose levels. However, these drugs may induce certain adverse effects, such as hypoglycemia (2,3). The consumption of anthocyanins (ANCs) has been suggested to be correlated with a reduced risk of degenerative diseases, such as atherosclerosis (4), cardiovascular diseases (5), cancer (6) and diabetes (7). ANCs extracted from *Calendula officinalis* fruits have been reported to enhance insulin release from pancreatic  $\beta$ -cells *in vitro* (8). Mulberry leaves and fruits have been used in the treatment of numerous diseases (9-12). The mulberry fruit (*Morus alba L.*, family Moraceae) contains abundant ANCs, which scavenge reactive oxygen species (13), have anti-obesity effects and inhibit low-density lipoprotein oxidation (14). The predominant ANCs in mulberry, cyanidin 3-rutinoside and cyanidin 3-glucoside, have been demonstrated to dose-dependently inhibit the migration and invasion of highly metastatic A549 human lung carcinoma cells (15). Furthermore, it was recently demonstrated that the cyanidin 3-O- $\beta$ -D-glucopyranoside fraction from mulberry fruit protected against bladder dysfunction in streptozotocin-induced diabetic rats (16). However, it has not yet been elucidated whether the ANCs in mulberry are able to significantly lower blood glucose levels and whether they may be useful in the treatment of the pathogenesis of type 2 diabetes.

---

**Correspondence to:** Dr Salunya Tancharoen, Department of Pharmacology, Faculty of Dentistry, Mahidol University, 6 Yothee Road, Rajthevee, Bangkok 10400, Thailand  
E-mail: salunya.tan@mahidol.ac.th

**Key words:** *Morus alba L.*, anthocyanins, type 2 diabetes, disease prevention

The evolution of diabetes in male leptin receptor-deficient Zucker diabetic fatty (ZDF) rats (ZDF/CrIcrlj) has resulted in it becoming a popular model for preclinical studies of type 2 diabetes, due to the fact that these rats exhibit disrupted islet architecture,  $\beta$ -cell degranulation and increased  $\beta$ -cell death (17,18). Therefore, ZDF male rats were used as a rodent model of type 2 diabetes in the present study. It was hypothesized that the consumption of an ANC extract from Thai *Morus alba* L. fruits was likely to result in glucose-lowering effects and enhanced insulin secretion. The purpose of this study was to determine the ANC composition of Thai *Morus alba* L. fruits, and to assess the effect of an ANC extract on the blood glucose and insulin levels in ZDF rats. To the best of our knowledge, the present study has demonstrated for the first time that ANCs extracted from Thai *Morus alba* L. have significant anti-diabetic activity. Furthermore, the ANC extract appeared to prevent the development of pathogenic lesions in diabetic islets by suppressing islet degeneration.

## Material and methods

**Plant material and extraction.** Mulberry fruits were obtained from Kamnan Jul Farm, Petchaboon Province, Thailand. The fruit was extracted in ethanol-water (50/50, v/v%), prior to the extract being filtered through a Buchner funnel and filter paper (Chmlab, Barcelona, Spain) and transferred to a 100 ml flask. The extract was then collected and condensed at 40°C using a Büchi B-490 rotary evaporator (Büchi Labortechnik AG, Flawil, Switzerland) under a vacuum and lyophilized with a freeze-dryer (Labconco Corp., Kansas City, MO, USA).

**Isolation and purification of mulberry ANCs.** A C18 Sep-Pak cartridge (Waters Corp., Milford, MO, US) was activated for 30 min with distilled water and high-performance liquid chromatography (HPLC)-grade methanol (Merck KGaA, Darmstadt, Germany). The ANC extract was then loaded onto the column. Following successive washes with five volumes of distilled water (acidified with 0.01% HCl) and ethyl acetate (Fisher Scientific UK Ltd., Loughborough, UK), the ANCs were eluted with methanol containing 0.01% HCl. The ANC solution was then collected and condensed at 40°C using a Büchi B-490 rotary evaporator under vacuum.

**HPLC-electrospray ionization (ESI)-mass spectrometry (MS).** ANCs in the partially purified extracts were separated and quantified by reverse-phase HPLC using a Hypersil™ Gold C18 column (inner diameter, 5  $\mu$ m; 4.6x250 mm; Thermo Fisher Scientific Inc., Salt Lake City, IL, USA). The column was eluted with a mobile phase consisting of water, 3.75% formic acid (VWR International, Ltd., Lutterworth, UK) and 15% methanol at a flow rate of 1 ml/min. The separated ANCs were detected and measured at 530 nm, and were identified based on the retention times and ultraviolet (UV)-visible (Vis) wavelength spectra of pure authentic standards (cyanidin 3-O-glucoside, cyanidin 3-rutinoside, pelargonidin 3-glucoside and pelargonidin 3-rutinoside; Sigma, St. Louis, MO, USA). The identity of each peak was verified by LC-MS (Agilent 1100; Agilent Technologies, Santa Clara, CA, USA) using ESI and operating in a single quadrupole mode.

The instrument was scanned over the *m/z* range of 200-1,500 in the ESI positive ion mode. The LC-MS was eluted with acetonitrile (Fisher Scientific UK Ltd.) and 0.5% ammonium hydroxide (90:10, v/v%).

**Quantification of ANCs by UV-Vis spectroscopy.** The ANCs were quantified by UV-Vis spectroscopy, as previously described (19). The model reaction solution was diluted with 0.01% HCl in distilled water and the absorbance at 510 nm was compared with that of known standard solutions using a Genesys 10 UV spectrophotometer (Thermo Spectronic, Rochester, NY, USA).

**Determination of total phenolic content.** The total phenolic content was determined using the Folin-Ciocalteu reagent (FCR), as previously described (20), with minor modifications. Briefly, 2.5 ml ethanolic mulberry extract was mixed with 0.5 ml FCR (Sigma) and 1.0 ml 20 g/100 g solution of sodium carbonate. The mixture was then incubated for 2 h in the dark at 25°C. The absorbance of the mixture was measured at 765 nm using a UV-Vis Genesys 10 UV spectrophotometer (Thermo Spectronic). A standard curve was plotted using gallic acid (0.07-10 mg/ml in methanol; Sigma) as a standard. The total phenolic content was expressed as gallic acid equivalents (GAEmM/Gfw). The assay was carried out in triplicate and the mean value was recorded.

**Determination of ferric-reducing antioxidant power (FRAP).** FRAP was measured as previously described (21). Briefly, FRAP reagent, which consisted of 0.3 M acetate buffer (pH 3.6), 10 mM 2,4,6-tris(2-pyridyl)-s-triazine (TPTZ) (Fluka, Buchs, Switzerland) in 40 mM HCl and 20 mM FeCl<sub>3</sub>.6H<sub>2</sub>O at a ratio of 10:1:1 (v/v/v) was freshly prepared prior to each measurement. Following this, 200  $\mu$ l mulberry extract was mixed with 1.3 ml FRAP reagent and incubated for 30 min at 37°C. The absorption was measured at 595 nm using an Epoch spectrophotometer (Bio-Tek Instruments, Inc. Winooski, VT, USA) with the Gen5 Data Analysis Software interface. Aqueous or methanol solutions containing known Fe(II) concentrations were used to calibrate the FRAP assay. FRAP values, expressed as mmol of Fe(II) equivalents (FeFmM/gFW), were determined by comparing the change in the absorption of the test mixture with that of the Fe(II) standards. The assay was carried out in triplicate and the mean value was recorded.

**Evaluation of the anti-diabetic effects of ANCs in ZDF rats.** Five-week-old male ZDF (Lepr<sup>fa</sup>/CrlCrlj) and age-matched lean rats (Lepr<sup>fa</sup>/±) were used in this study. All rats were ordered as bred from Charles River Laboratories International (Wilmington, MA, USA). All animal studies were conducted according to the National Institutes of Health Guidelines for the Care and Use of Animals, and were reviewed and approved by the Committee on Animal Experimentation of Kagoshima University (Kagoshima, Japan). The rats were kept under pathogen-free conditions with a 12-h light-dark cycle (lights on at 07:00) at 22±1°C.

The ZDF and lean rats were treated with 125 or 250 mg ANCs/body weight dissolved in 1% CMC (Sigma) in distilled water by gavage, twice daily. The control groups received 1% carboxymethylcellulose (CMC) in distilled water alone.

Following the allocation of the rats to each experimental group, the rats were left to acclimatize and were fed a control diet for 1 week. Food was then withheld for 24 h and tail vein blood samples were collected subsequent to cutting the tip of the tail with a scalpel. The blood samples were centrifuged, and the plasma was stored at  $-20^{\circ}\text{C}$  until assay. Blood glucose levels were monitored every week using a glucose meter (Accu-Chek<sup>®</sup> Active; Roche Diagnostics). Following 5 weeks of treatment with ANCs or CMC, the rats were sacrificed by heart puncture using sterile needles and syringes under anesthesia with diethyl ether, and blood was collected. Plasma insulin levels were measured using an enzyme immunoassay (Cayman Chemical Co., Ann Arbor, MI, USA). All experiments were performed using conscious unrestrained rats.

Following the sacrifice of the rats, the pancreas was perfused with physiological saline and rapidly excised. The tissue samples were maintained in 10% neutral-buffered formalin, dehydrated in a graded ethanol series, cleared in xylene and embedded in paraffin wax. Sections ( $4\ \mu\text{m}$  thick) were stained with hematoxylin and eosin (H&E). For histological analysis, the tissue sections were photographed using a high-resolution color digital camera mounted on an Olympus BX51 microscope (Olympus, Tokyo, Japan), and the images were transferred to a computer. Four sections were examined from each animal in each treatment group.

**Cell culture and treatment.** Murine macrophage-like cells (RAW 264.7) and rat renal tubular epithelial cells (NRK-52E) were obtained from the American Type Culture Collection (Manassas, VA, USA). RAW 264.7 cells were maintained in RPMI-1640 medium (Gibco BRL, Grand Island, NY, USA) supplemented with 10% fetal bovine serum and 2 mmol/l glutamine (Hyclone, Logan, UT, USA). NRK-52E cells were grown in Dulbecco's modified Eagle's medium (DMEM; Gibco BRL) containing 7% (v/v) fetal bovine serum and 2 mmol/l glutamine (Hyclone). RAW 264.7 cells ( $3.5 \times 10^4$  cells/well) and NRK-52E cells ( $4 \times 10^4$  cells/well) were cultured in serum-free Opti-MEM<sup>®</sup> I medium (Gibco BRL) and serum-free DMEM, respectively, prior to stimulation with various concentrations (0, 2, 10, 30, 50 or 100  $\mu\text{g}/\text{ml}$ ) of mulberry extract for 24 h.

**Methylthiazolyl-diphenyl-tetrazolium bromide (MTT) assay.** Cell viability was assessed using a modified MTT assay. Briefly, following the exposure of the cells to the specified concentration of mulberry extract for 48 h, MTT solution was added to each well of the six-well plate. Three hours subsequently, dimethyl sulfoxide (DMSO) was added and the plate was incubated for 24 h at  $37^{\circ}\text{C}$ . Absorbance was measured at 570 nm using an automatic microplate reader (ImmunoMini NJ-2300; InterMed, Tokyo, Japan).

**Statistical analysis.** Data were analyzed using SPSS statistical software version 3.0 (SPSS, Inc., Chicago, IL, USA). Data are shown as the mean  $\pm$  standard deviation. The significance of the differences between two groups was assessed using the Student's t-test, and differences between multiple groups were assessed by one-way analysis of variance (ANOVA) followed by the Scheffé's multiple range test. Values of  $P < 0.05$  were considered to indicate a statistically significant difference.

## Results

**Analysis of mulberry ANCs.** The ANC composition of mulberry fruit was determined by HPLC-ESI-MS. The ANC extract was purified using a C-18 Sep-Pak cartridge, and the resulting chromatogram, at 520 nm, is shown in Fig. 1. The chromatogram contained four peaks within the retention time of 31-38 min, indicating the presence of four different ANCs in mulberry fruit (Table I). Peak 1, with a retention time of 31.3 min,  $\text{M}^+$  at  $m/z$  449.1 and a fragment ion at  $m/z$  287.0, was identified as cyanidin 3-O-glucoside (51.4%). Peak 2, with a retention time of 33.0 min,  $\text{M}^+$  at  $m/z$  595.2 and fragment ions at  $m/z$  449.1 and 287.0, was identified as cyanidin 3-rutinoside (45.3%). Peak 3, with a retention time of 36.4 min,  $\text{M}^+$  at  $m/z$  433.1 and a fragment ion at  $m/z$  271.0, was identified as pelargonidin 3-glucoside (2.1%). Peak 4, with a retention time of 38.0 min,  $\text{M}^+$  at  $m/z$  579.1 and fragment ions at  $m/z$  433.1 and 271.0, was identified as pelargonidin 3-rutinoside (1.2%). The results of the UV-Vis quantification of the total ANC content showed that the phenolic-rich extract contained 28 mg/g of total ANCs (calculated as cyanidin-3-O-glucoside equivalents). The total phenolic content of ANC extracts, expressed as mmol of Fe(II) equivalents and gallic acid equivalents, was 67.28 GAEmM/Gfw and 22.67 FeFmM/gFW, respectively (data not shown).

**Hypoglycemic effects of ANCs and histology of pancreatic islets in ZDF rats.** Table II shows the changes in body weight observed in the six groups of rats. The ZDF rats had significantly higher body weights than their lean littermates from 8 weeks of age, and the body weight progressively increased with age ( $P < 0.05$ ). ANC treatment did not affect body weight in either genotype. Moreover, following 4 weeks of treatment, ZDF rats treated with 250 mg/kg ANCs tended to gain more weight than those treated with CMC alone or with 125 mg/kg ANCs, although this was not statistically significant ( $P = 0.3$  versus CMC;  $P = 0.11$  versus 125 mg/kg ANCs).

Blood glucose levels were measured in all of the rats for 5 weeks prior to the commencement of the study and throughout the experimental period (Fig. 2A). At 7 weeks of age, the ZDF rats treated with the vehicle showed mild hyperglycemia ( $\sim 159$  mg/dl) that rapidly progressed, reaching levels of  $\sim 396$  mg/dl after 3 weeks. The administration of ANCs did not affect the glucose levels in the lean rats. Glucose levels increased significantly from  $105.5 \pm 8.7$  mg/dl at 0 weeks to  $396.25 \pm 21$  mg/dl ( $P < 0.0001$ ) at 5 weeks in the ZDF rats treated with CMC; however, the glucose levels were significantly lower in the rats treated with 125 and 250 mg/kg ANCs ( $228.25 \pm 45$  and  $131.75 \pm 10$  mg/dl, respectively;  $P < 0.001$  for each; Fig. 2B). Treatment with 250 mg/kg ANCs reduced glucose levels in the ZDF rats to values similar to those in their lean littermates (Fig. 2).

At the start of treatment, when the rats were 5 weeks of age, plasma insulin levels were significantly higher in the ZDF rats than in the lean rats ( $11 \pm 0.2$  versus  $4.2 \pm 0.0$  pg/ml;  $P < 0.001$ ; Fig. 3). Between 0 and 5 weeks, the insulin levels decreased from  $10.88 \pm 0.0$  to  $7.9 \pm 0.4$  ng/ml ( $P < 0.05$ ) in the CMC-treated ZDF rats, and from  $11.51 \pm 0.0$  to  $8.72 \pm 1.4$  ng/ml ( $P < 0.05$ ) in the ZDF rats treated with 125 mg/kg ANCs. Notably, plasma insulin levels did not decrease in the ZDF rats treated

Table I. Identification of anthocyanins (ANCs) in mulberry fruit.

Compound number <sup>a</sup>	Retention time (min)	MS, M+ ( <i>m/z</i> )	MS/MS ( <i>m/z</i> )	Assignment <sup>b</sup>
1	31.3	449.1	287.0	Cyanidin 3-O-glucoside
2	33.0	595.2	449.1/287.0	Cyanidin 3-rutinoside
3	36.4	433.1	271.0	Pelargonidin 3-glucoside
4	38.0	579.1	433.1/271.0	Pelargonidin 3-rutinoside

<sup>a</sup>Diode array detection at 350 nm; <sup>b</sup>Based on the fragmentation pattern and its aglycone. The assay was performed in triplicate. MS, mass spectrometry.

Table II. Changes in body weight in each experimental group.

Group	Body weight (g)			
	0 weeks	2 weeks	4 weeks	5 weeks
Lean rats				
+1% CMC	124±6	152±2	226±6	277±10
+125 ANCs	121±13	153±6	226±4	288±15
+250 ANCs	118±5	149±7	211±11	270±13
ZDF rats				
+1% CMC	143±2	182±4	256±30	324±24
+125 ANCs	139±3	187±6	257±9	317±34
+250 ANCs	140±6	188±6	273±15	331±7

ZDF, Zucker diabetic fatty; +1% CMC, treated with 1% carboxymethylcellulose; +125 ANCs, treated with 125 mg anthocyanins/kg body weight; +250 ANCs, treated with 250 mg anthocyanins/kg body weight.

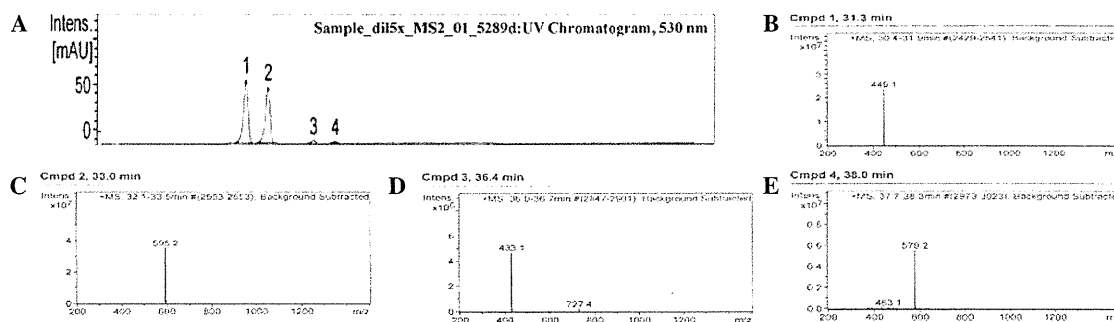


Figure 1. High-performance liquid chromatography (HPLC)-electrospray ionization (ESI)-mass spectrometry (MS) analysis of mulberry anthocyanins (ANCs). (A) Chromatogram for the ANC extract of mulberry fruit at 520 nm. Four peaks were detected with retention times ranging from 31 to 38 min. Chromatograms for (B) cyanidin 3-O-glucoside, (C) cyanidin 3-rutinoside, (D) pelargonidin 3-glucoside and (E) pelargonidin 3-rutinoside. The parameters used for peak identification are listed in Table I. Intens, intensity; Cmpd, compound.

with 250 mg/kg ANCs (0 weeks: 10.8±0.6 ng/ml; 5 weeks: 10.93±0.4 ng/ml).

A histological evaluation of the pancreatic islets of 10-week-old ZDF and lean rats was also conducted. H&E staining revealed no significant pathological abnormalities in the islets from the lean rats, which were round or oval with well-defined boundaries (Fig. 4A-C). However, histological examination of the pancreatic islets from the CMC-treated ZDF rats revealed substantial changes in islet

morphology. In particular, the islets were hypertrophic and compressed adjacent exocrine tissue, and there was marked vascular congestion or hemorrhagic degeneration (Fig. 4D, upper panel). Furthermore, the islets were disorganized, with finger-like projections into the surrounding exocrine tissue. The degenerated islets also showed  $\beta$ -cell vacuolation and degeneration (Fig. 4D, lower panel). By contrast, the histological assessment of pancreatic sections from the ZDF rats treated with 125 mg/kg ANCs showed a normal distribution

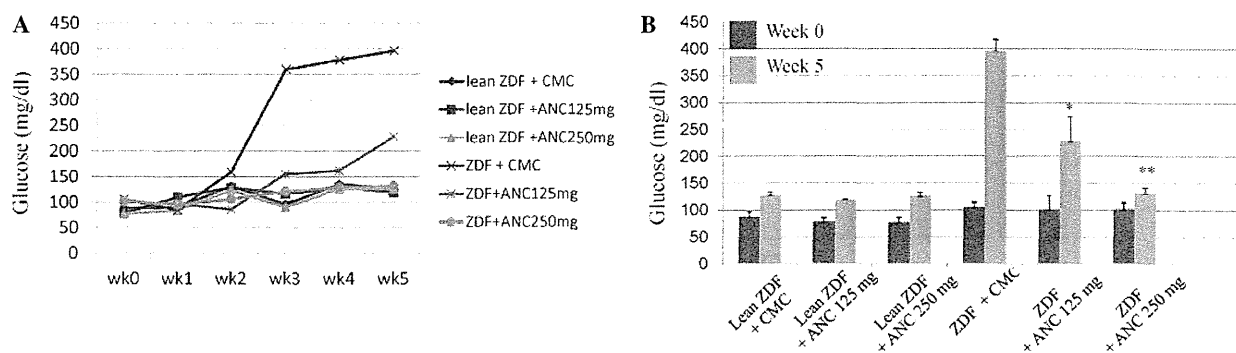


Figure 2. Blood glucose levels of Zucker diabetic fatty (ZDF) and lean ZDF rats treated with 125 or 250 mg/kg anthocyanin (ANC) or 1% carboxymethylcellulose (CMC; vehicle control). (A) Blood glucose levels measured every week during the experimental period. ANCs lowered the glucose levels in the ZDF rats within 3 weeks of treatment in comparison with the levels in the CMC-treated rats. (B) Change in glucose levels from week 0 to week 5. The results are shown as the mean  $\pm$  standard deviation (n=3-5 rats/group). \*P<0.001 and \*\*P<0.0001 vs. CMC-treated ZDF rats.

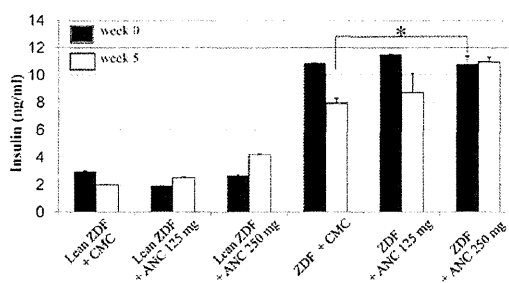


Figure 3. Plasma insulin levels in Zucker diabetic fatty (ZDF) and lean ZDF rats treated with 125 or 250 mg/kg anthocyanin (ANC) or 1% carboxymethylcellulose (CMC) for 5 weeks. Plasma insulin levels at week 0 were significantly higher in the ZDF rats than in their lean littermates (P<0.001). The insulin secretion in the 250 mg/kg ANC-treated ZDF rats at week 5 was 27% higher than that in the CMC-treated ZDF rats. The results are shown as the mean  $\pm$  standard deviation (n=3-5 rats/group). \*P<0.001.

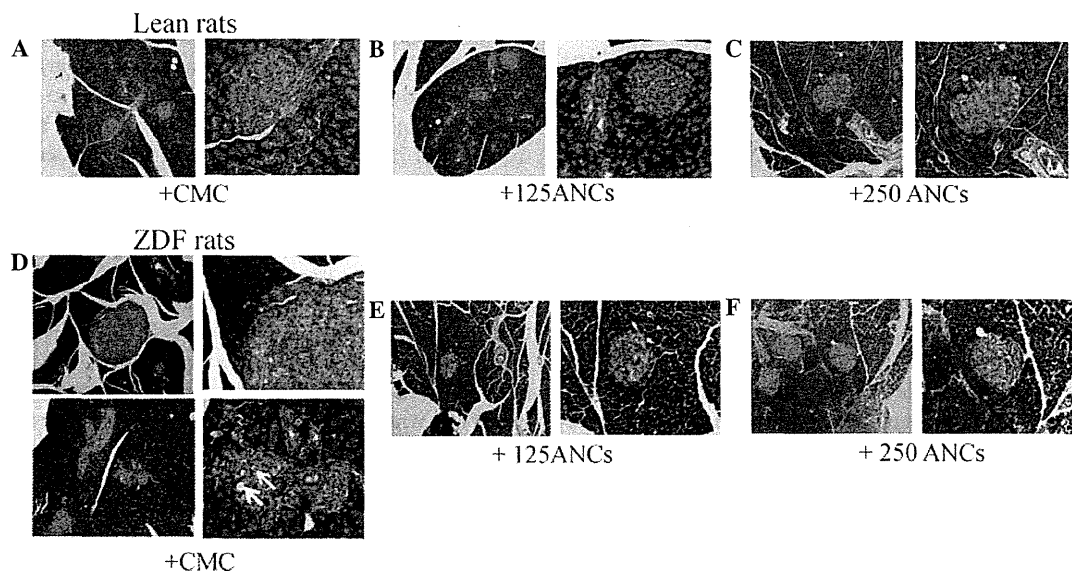


Figure 4. Representative hematoxylin/eosin (H&E)-stained pancreas tissue sections from 11-week-old obese Zucker diabetic fatty (ZDF) and lean rats treated with 125 or 250 mg/ml anthocyanin (ANC) or 1% carboxymethylcellulose (CMC). (A-C) There were no pathological abnormalities in the islets of lean rats. The islets consisted of small, rounded aggregates of mildly eosinophilic cells and were regularly shaped with well-defined boundaries. (D) There were marked morphological changes in the islets of obese ZDF rats, as the islets were hypertrophied and compressed adjacent exocrine tissue, resulting in vascular congestion and hemorrhage. The islets were also disorganized, with extensions into the surrounding exocrine tissue. The degenerated islets showed  $\beta$ -cell vacuolation and degeneration (arrows). (E) Islets of ZDF rats treated with 125 mg/kg ANC showed a normal distribution within the exocrine tissue and mild  $\beta$ -cell vacuolation. (F) There were substantially fewer degenerated islets in ZDF rats treated with 250 mg/kg ANC. The islets in these rats were regularly shaped with well-defined boundaries. H&E staining; original magnification, x100 (left image) and x200 (right image).

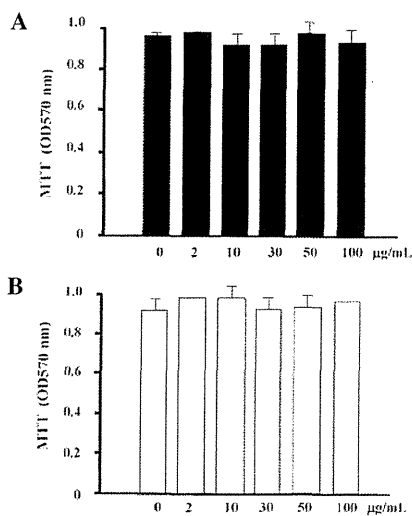


Figure 5. Cytotoxic effect of anthocyanins (ANCs) on (A) murine macrophages and (B) rat kidney cells. Cells were exposed to the indicated concentration of ANC for 48 h and cell viability was quantified using an MTT assay. The results are shown as the mean  $\pm$  standard deviation for two separate experiments, with each condition performed in duplicate.

of islets within the exocrine tissue and some  $\beta$ -cell vacuolation (Fig. 4E). Notably, the evaluation of the pancreatic tissue samples collected from the ZDF rats treated with 250 mg/kg ANCs suggested that this dose had certain protective effects, since there were fewer abnormal morphological features and fewer degenerated islets. Additionally, the islets demonstrated a regular shape with well-defined boundaries (Fig. 4F).

In the cell culture studies, it was observed that the ANCs did not exert any cytotoxic effects on the murine macrophages or rat kidney cells (Fig. 5).

## Discussion

The results from this study suggest that ANCs extracted from mulberry fruit exhibit significant anti-diabetic properties by improving blood glucose levels in ZDF rats as an animal model of type 2 diabetes. To the best of our knowledge, this has shown for the first time that ANCs are able to attenuate islet degeneration in ZDF rats. The results demonstrating that ANCs reduced blood glucose levels were consistent with those of a prior study showing that ANCs extracted from black soybean seed coats exhibited antidiabetic and antioxidative effects in streptozotocin-induced diabetic rats (22). Furthermore, the administration of ANCs extracted from *Calendula officinalis* fruits has been demonstrated to significantly increase insulin release from pancreatic  $\beta$ -cells *in vitro* (8).

In the present study, the chromatogram of the purified product following acid hydrolysis of the ethanol extract revealed that cyanidin 3-O-glucoside (51.4%) and cyanidin-3-rutinoside (45.3%) were the major ANCs present in Thai *Morus alba L.* The minor ANCs, which comprised 3.3% of the total ANCs, were pelargonidin 3-O-glucoside and pelargonidin 3-O-rutinoside. These results were consistent with those revealed in the study by Qin *et al.* (23), although the ANC content differed, most likely due to differences

between mulberry species and cultivars, as well as differences in extraction, separation, purification and analysis between the two studies.

Lean ZDF rats have been demonstrated to be less sensitive to exogenous glucose-induced hyperglycemia (23). The ZDF rats in the present study exhibited marked hyperglycemia at 7 weeks of age and their blood glucose levels continued to increase with age. These results were consistent with those of a previous study in which diabetes occurred spontaneously in male rats aged  $\sim$ 6 weeks, and was associated with hyperphagia, polyuria and polydipsia (24). It was also revealed that the  $\beta$ -cell mass decreased by 51% from 9 to 12 weeks of age (24). In rats aged 6-12 weeks, the  $\beta$ -cell mass is not able to compensate for insulin resistance, resulting in compensatory  $\beta$ -cell proliferation (25).

In a previous study, treatment with the ANC cyanidin 3-O-glucoside reduced the body weight and fat accumulation in visceral adipose and liver tissues of KK-Ay mice by improving triglyceride metabolism and regulating lipoprotein lipase activity (26). In another study, aqueous mulberry extract exhibited anti-obesity effects by upregulating hepatic peroxisome proliferator-activated receptor  $\alpha$  and carnitine palmitoyltransferase-1 expression, and reducing fatty acid synthase and 3-hydroxy-3-methylglutaryl-coenzyme A (HMG-CoA) reductase expression (14). However, in the present study, the ANC extract from mulberry fruit did not promote reductions in body weight. In fact, the dose of 250 mg/kg ANCs resulted in a certain level of weight gain in the ZDF rats from the age of 9 weeks ( $P > 0.05$ ), without changes in food intake. The differences in results may be due to differences in the polyphenols contained in the extracts or their free radical scavenging properties and mechanisms of action.

To the best of our knowledge, this study has demonstrated for the first time that mulberry fruit extract contains abundant cyanidin 3-O-glucoside ( $\sim$ 28 mg/g of crude ANC extract), with the highest ANC dose (250 mg/kg body weight) containing  $\sim$ 7 mg cyanidin 3-O-glucoside. Blood glucose levels were 66% lower and insulin levels were 27% higher in the ZDF rats treated with 250 mg/kg ANCs than in those treated with CMC between 5 and 10 weeks of age. In addition, the consumption of ANCs did not affect glycemia in lean rats. The maximum dose of ANCs used in this study was derived from the cyanidin 3-O-glucoside concentration (10 mg/kg) used in a prior study (11). To date, there are limited data on the mechanisms of ANCs with regard to insulin-mediated glucose uptake. Certain studies have shown that cyanidin 3-O-glucoside from black beans significantly upregulated glucose transport 4 (GLUT4) expression, induced adipocyte differentiation and glucose uptake *in vitro* (27), and prevented insulin resistance and pancreatic apoptosis in streptozotocin-induced diabetic rats (28).

In the present study, the islets of the lean rats showed normal histological features. By contrast, there were marked morphological changes, including islet hypertrophy and cellular degeneration, in the CMC-treated ZDF rats. These pathological observations were consistent with those of earlier studies showing pancreatic islet hypertrophy in ZDF rats (29). By the time diabetes is diagnosed,  $\beta$ -cells attempt to secrete sufficient insulin to overcome the insulin resistance in a process that involves islet hyperplasia. Degenerating islet

cells show cytoplasmic vacuolation, possibly resulting from autodigestion following cell death (25). In the present study, the histological assessment of the pancreatic islets from the ZDF rats demonstrated that 250 mg/kg ANCs attenuated the degenerative changes in the majority of the rats. Furthermore, the ANC extract prevented marked reductions in the plasma insulin levels in these rats. These effects may be coupled with enhanced hepatic/peripheral tissue glucose uptake. It was not possible to clarify the mechanism from the current results. Further studies are required to identify the mechanisms of action of ANCs using isolated islets or  $\beta$ -cells to examine whether ANCs have direct effects on insulin secretion.

In conclusion, our results suggest that the ANC extract of mulberry fruit is an effective anti-diabetic agent with marked glucose-lowering effects that prevents the progressive decline in insulin secretion. Although ANCs may protect against  $\beta$ -cell damage, further studies are required to examine the pharmacokinetics and the molecular basis for the pharmacological activity of ANCs on insulin resistance and glucose handling in the management of diabetes mellitus. Long-term studies are required to confirm the present results and to establish the durability of the improvements in glucose levels.

#### Acknowledgements

This study was supported in part by a grant from the SENSHIN Medical Research Foundation. The authors would like to thank Ms. Pornpen Dararat, Dr Yuko Nawa, Dr Fumiyo Masuda, Ms. Tomoka Nagasato, Ms. Mika Yamamoto, Ms. Nobue Uto and all the staff at the Department of Laboratory and Vascular Medicine, Kagoshima University (Kagoshima, Japan) and the Department of Pharmacology, Faculty of Dentistry, Mahidol University (Bangkok, Thailand), for their assistance with the experiments.

#### References

- Jun H, Bae HY, Lee BR, *et al*: Pathogenesis of non-insulin-dependent (type II) diabetes mellitus (NIDDM) - genetic predisposition and metabolic abnormalities. *Adv Drug Deliv Rev* 35: 157-177, 1999.
- Rosak C: The pathophysiologic basis of efficacy and clinical experience with the new oral antidiabetic agents. *J Diabetes Complications* 16: 123-132, 2002.
- Jennings AM, Wilson RM and Ward JD: Symptomatic hypoglycemia in NIDDM patients treated with oral hypoglycemic agents. *Diabetes Care* 12: 203-208, 1989.
- Xia X, Ling W, Ma J, *et al*: An anthocyanin-rich extract from black rice enhances atherosclerotic plaque stabilization in apolipoprotein E-deficient mice. *J Nutr* 136: 2220-2225, 2006.
- Wallace TC: Anthocyanins in cardiovascular disease. *Adv Nutr* 2: 1-7, 2011.
- Wang LS and Stoner GD: Anthocyanins and their role in cancer prevention. *Cancer Lett* 269: 281-290, 2008.
- Grace MH, Ribnicky DM, Kuhn P, *et al*: Hypoglycemic activity of a novel anthocyanin-rich formulation from lowbush blueberry, *Vaccinium angustifolium* Aiton. *Phytomedicine* 16: 406-415, 2009.
- Jayaprakasam B, Vareed SK, Olson LK and Nair MG: Insulin secretion by bioactive anthocyanins and anthocyanidins present in fruits. *J Agric Food Chem* 53: 28-31, 2005.
- Duthie G and Crozier A: Plant-derived phenolic antioxidants. *Curr Opin Clin Nutr Metab Care* 3: 447-451, 2000.
- Kaewkaen P, Tong-Un T, Wattanathorn J, *et al*: Mulberry fruit extract protects against memory impairment and hippocampal damage in animal model of vascular dementia. *Evid Based Complement Alternat Med* 2012: 263520, 2012.
- Andallu B, Kumar AV and Varadacharyulu NC: Oxidative stress in streptozocin-diabetic rats: Amelioration by mulberry (*Morus Indica* L.) leaves. *Chin J Integr Med Dec*. 22, 2012 (Epub ahead of print).
- Musabayane CT, Bwititi PT and Ojewole JA: Effects of oral administration of some herbal extracts on food consumption and blood glucose levels in normal and streptozotocin-treated diabetic rats. *Methods Find Exp Clin Pharmacol* 28: 223-228, 2006.
- Du Q, Zheng J and Xu Y: Composition of anthocyanins in mulberry and their antioxidant activity. *J Food Compos Anal* 21: 390-395, 2008.
- Peng CH, Liu LK, Chuang CM, Chyau CC, Huang CN and Wang CJ: Mulberry water extracts possess an anti-obesity effect and ability to inhibit hepatic lipogenesis and promote lipolysis. *J Agric Food Chem* 59: 2663-2671, 2011.
- Chen PN, Chu SC, Chiou HL, Kuo WH, Chiang CL and Hsieh YS: Mulberry anthocyanins, cyanidin 3-rutinoside and cyanidin 3-glucoside, exhibited an inhibitory effect on the migration and invasion of a human lung cancer cell line. *Cancer Lett* 235: 248-259, 2006.
- Ha US, Bae WJ, Kim SJ, *et al*: Protective effect of cyanidin-3-O- $\beta$ -D-glucopyranoside fraction from mulberry fruit pigment against oxidative damage in streptozotocin-induced diabetic rat bladder. *NeuroUrol Urodyn* Nov. 25, 2012 (Epub ahead of print).
- Clark JB, Palmer CJ and Shaw WN: The diabetic Zucker fatty rat. *Proc Soc Exp Biol Med* 173: 68-75, 1983.
- Mega C, de Lemos ET, Vala H, *et al*: Diabetic nephropathy amelioration by a low-dose sitagliptin in an animal model of type 2 diabetes (Zucker diabetic fatty rat). *Exp Diabetes Res* 2011: 162092, 2011.
- Yu X, Zhao M, Hu J, Zeng S and Bai X: Correspondence analysis of antioxidant activity and UV-Vis absorbance of Maillard reaction products as related to reactants. *LWT - Food Science and Technology* 46: 1-9, 2012.
- Zhang M, Chen H, Li J, Pei Y and Liang Y: Antioxidant properties of tartary buckwheat extracts as affected by different thermal processing methods. *LWT - Food Science and Technology* 43: 181-185, 2010.
- Sutharut J and Sudarat J: Total anthocyanin content and antioxidant activity of germinated colored rice. *International Food Research Journal* 19: 215-221, 2012.
- Nizamutdinova IT, Jin YC, Chung JI, *et al*: The anti-diabetic effect of anthocyanins in streptozotocin-induced diabetic rats through glucose transporter 4 regulation and prevention of insulin resistance and pancreatic apoptosis. *Mol Nutr Food Res* 53: 1419-1429, 2009.
- Qin C, Li Y, Niu W, Ding Y, Zhang R and Shang X: Analysis and characterisation of anthocyanins in mulberry fruit. *Czech J Food Sci* 28: 117-126, 2010.
- Jones HB, Nugent D and Jenkins R: Variation in characteristics of islets of Langerhans in insulin-resistant, diabetic and non-diabetic-rat strains. *Int J Exp Pathol* 91: 288-301, 2010.
- Pick A, Clark J, Kubstrup C, Levisetti M, Pugh W, Bonner-Weir S and Polonsky KS: Role of apoptosis in failure of beta-cell mass compensation for insulin resistance and beta-cell defects in the male Zucker diabetic fatty rat. *Diabetes* 47: 358-364, 1998.
- Wei X, Wang D, Yang Y, *et al*: Cyanidin-3-O- $\beta$ -glucoside improves obesity and triglyceride metabolism in KK-Ay mice by regulating lipoprotein lipase activity. *J Sci Food Agric* 91: 1006-1013, 2011.
- Inaguma T, Han J and Isoda H: Improvement of insulin resistance by Cyanidin 3-glucoside, anthocyanin from black beans through the up-regulation of GLUT4 gene expression. *BMC Proc* 5 (Suppl 8): P21, 2011.
- Nizamutdinova IT, Jin YC, Chung JI, Shin SC, Lee SJ, Seo HG, Lee JH, Chang KC and Kim HJ: The anti-diabetic effect of anthocyanins in streptozotocin-induced diabetic rats through glucose transporter 4 regulation and prevention of insulin resistance and pancreatic apoptosis. *Mol Nutr Food Res* 53: 1419-1429, 2009.
- Janssen SW, Hermus AR, Lange WP, *et al*: Progressive histopathological changes in pancreatic islets of Zucker Diabetic Fatty rats. *Exp Clin Endocrinol Diabetes* 109: 273-282, 2001.



# Upregulation of non- $\beta$ Cell-derived Vascular Endothelial Growth Factor A Increases Small Clusters of Insulin-producing Cells in the Pancreas

**One Sentence Summary:** The authors showed that upregulation of non-beta cell-derived VEGF-A increased the number of small clusters of insulin producing cells without forming islets in mice, which suggests new functions of non-beta cell-derived VEGF-A to insulin producing cell regeneration and insulin production.

## Authors

K. Takenouchi<sup>1</sup>, B. Shrestha<sup>1</sup>, M. Yamakuchi<sup>1</sup>, N. Yoshinaga<sup>2</sup>, N. Arimura<sup>2</sup>, H. Kawaguchi<sup>3</sup>, T. Nagasato<sup>4</sup>, R. Feil<sup>5</sup>, K.-i. Kawahara<sup>6</sup>, T. Sakamoto<sup>2</sup>, I. Maruyama<sup>4</sup>, T. Hashiguchi<sup>1</sup>

## Affiliations

Affiliation addresses are listed at the end of the article

## Key words

- ◉ diabetes
- ◉ islet
- ◉ smooth muscle cell
- ◉ streptozotocin

## Abstract



**Background:** Pancreatic  $\beta$  cell-derived vascular endothelial growth factor A (VEGF-A) contributes to normal  $\beta$  cell function. We therefore hypothesized that non- $\beta$  cell-derived VEGF-A may affect its properties in adult mice.

**Methods:** We generated transgenic mice expressing human VEGF-A (hVEGF-A) in a visceral smooth muscle cell (SMC)-dominant manner under the control of the transgelin (*Tagln/SM22 $\alpha$* ) promoter via a tamoxifen-induced Cre/loxP recombination system (SM-CreER<sup>T2</sup>/hVEGF mice).

SM-CreER<sup>T2</sup>/hVEGF mice received tamoxifen orally followed by microscopic examination of their pancreas 4 weeks after the hVEGF-A induction. The number of clusters of insulin-producing cells (IPCs) in islets, pancreatic ducts, and individual IPCs were counted.

**Results:** The number of small IPC clusters (100–215  $\mu\text{m}^2$ ) in the pancreas increased signifi-

cantly in SM-CreER<sup>T2</sup>/hVEGF mice compared to SM-CreER<sup>T2</sup>(Ki) mice (473 out of 1 992 counts vs. 199 out of 976 counts,  $p < 0.05$ ), although total IPC area and the number of pancreatic duct IPCs, in proportion to exocrine area, were similar between the 2 groups. Although most small IPC clusters observed in SM-CreER<sup>T2</sup>/hVEGF mice were not accompanied by  $\alpha$  and/or  $\delta$  cells, some were attached to a single or a few  $\alpha$  cells. An STZ-induced diabetic state in SM-CreER<sup>T2</sup>/hVEGF mice was slightly ameliorated, with only one point of significance 12 weeks after STZ administration, compared to SM-CreER<sup>T2</sup>(Ki) mice.

**Conclusion:** Upregulation of non- $\beta$  cell-derived VEGF-A may alter the composition of pancreatic IPCs by increasing the number of small IPC clusters. These findings provide new information on the role of non- $\beta$  cell-derived VEGF-A to IPC regeneration and insulin production.

received 06.02.2014  
first decision 06.02.2014  
accepted 26.02.2014

## Bibliography

DOI <http://dx.doi.org/10.1055/s-0034-1371811>  
Exp Clin Endocrinol Diabetes 2014; 122: 1–8  
© J. A. Barth Verlag in Georg Thieme Verlag KG Stuttgart · New York  
ISSN 0947-7349

## Correspondence

**T. Hashiguchi, MD, PhD**  
Department of Laboratory and Vascular Medicine  
Kagoshima University Graduate School of Medical and Dental Sciences  
8-35-1, Sakuragaoka  
Kagoshima 890-8520  
Japan  
Tel.: +81/99/275/5437  
Fax: +81/99/275/2629  
terutoha@m3.kufm.  
kagoshima-u.ac.jp

## Introduction



Several studies have demonstrated a relationship between islet vascularization and function. Normal islets are highly vascularized and contain fenestrated endothelium. During embryonic development, the pancreatic endothelium signals pancreatic islets to develop. Subsequently, islet cells signal back to the vascular endothelium to form a branching network of capillaries in the growing islets [1]. Because vascular endothelial growth factor A (VEGF-A) is a key molecule for angiogenesis, the role of VEGF-A in islet vascularization has been studied intensively. Lammert et al. reported that VEGF-A was not required for the development of islet capillaries, but that it induced a capillary network essential for the fine-tuning of blood glucose regulation [2]. In addition, Brissova et al. showed that VEGF-A was

a major regulator of islet vascularization and revascularization of transplanted islets [3]. Islet VEGF-A expression is thus thought to be essential for maintaining normal islet vascularization and function. Although most of these experiments have been conducted using a  $\beta$ -cell-specific VEGF-A-deficient/over expression model, the biological effect of upregulated non- $\beta$  cell-derived VEGF-A on its properties in vivo has not been investigated. Therefore, we generated transgenic mice expressing hVEGF-A in a visceral smooth muscle cell (SMC)-dominant manner, under the control of the transgelin (*Tagln/SM22 $\alpha$* ) promoter and a tamoxifen-induced Cre/loxP recombination system (SM-CreER<sup>T2</sup>/hVEGF mice) [4], to examine its role in the pancreas. Using these mice, we demonstrate that upregulation of non- $\beta$  cell-derived VEGF-A increased the number of small clusters of IPCs without forming islets,

which suggests new functions of non- $\beta$  cell-derived VEGF-A to IPC regeneration and insulin production.

## Materials and Methods

### Animals

Mice were kept in environmentally controlled pathogen-free conditions (lights on from 7:00 to 19:00; 23°C; 55% humidity) with ad libitum access to water and a standard rodent diet. Animal experiments were performed according to the guidelines of the Natural Science Center for Research and Education, Kagoshima University. SM-CreER<sup>T2</sup> (ki) mice carrying a *Tagln* knock-in allele, which expresses CreER<sup>T2</sup> recombinase in response to tamoxifen administration, instead of the endogenous *Tagln* gene, were provided by Dr. Robert Feil [5].

### Establishment of SM-CreER<sup>T2</sup>/hVEGF mice

The plasmid construct containing human *VEGFA* flanked by a second *loxP* site (p-hVEGF-A<sup>fl</sup>) is shown in **Fig. 1**. To construct p-hVEGF-A<sup>fl</sup>, the *lacZ* gene in pCETZ-17 was replaced by a 576-bp cDNA encoding human *VEGFA* [6]. The resulting DNA construct (p-hVEGF-A<sup>fl</sup>) contained a CMV enhancer/chicken  $\beta$ -actin promoter (CAG), and an enhanced green fluorescent protein (EGFP)/chloramphenicol acetyltransferase (CAT) flanked by 2 *loxP* sites. The 5.4-kb *Spe I* fragment containing the hVEGF-A<sup>fl</sup> transgene was removed from the p-hVEGF-A<sup>fl</sup> vector and micro-injected into fertilized egg pronuclei from C57BL/6N mice [6].

Transgenic founder (F0) mice (hVEGF-A<sup>fl</sup> mice) were identified by EGFP-fluorescent blood cells using flow cytometry [7].

The presence of the hVEGF-A<sup>fl</sup> transgene was confirmed by PCR with primers *Chi5'* (5'-GGC GGG GTT CGG CTT CTG GCG TGT GAC CGG-3') and *Veg3'* (5'-TCA CCG CCT CGG CTT GTC ACA TCT GCA AGT-3'), which recognize the chicken  $\beta$ -actin promoter and *VEGFA*, respectively. All F0 transgenic mice were crossed with wild-type C57BL/6N mice (aged 12–20 weeks). SM-CreER<sup>T2</sup> (ki) mice were mated with heterozygous hVEGF-A<sup>fl</sup> mice to generate double transgenic offspring expressing Cre, which would then respond to tamoxifen administration in an SMC-specific manner (SM-CreER<sup>T2</sup>/hVEGF mice).

### Preparation and administration of tamoxifen

A 10-mg/mL tamoxifen stock solution for intraperitoneal injection was prepared and stored as described previously [4]. Tamoxifen-containing chow (200 mg/kg food) was prepared by mixing 100 g of powdered mouse food and 20 mg of ground tamoxifen tablets (AstraZeneca PLC, London, UK) before use. Mice were injected with 100  $\mu$ L of tamoxifen stock solution (1 mg tamoxifen) intraperitoneally for 5 days or fed tamoxifen-supplemented diet for 5 days.

### Blood analysis

Blood samples were obtained from the saphenous vein as described previously [8]. Mice were fasted for 8 h before measuring fasting blood glucose levels using an enzyme-electrode method (Glutest; Sanwa Kagaku Kenkyusho, Nagoya, Japan).

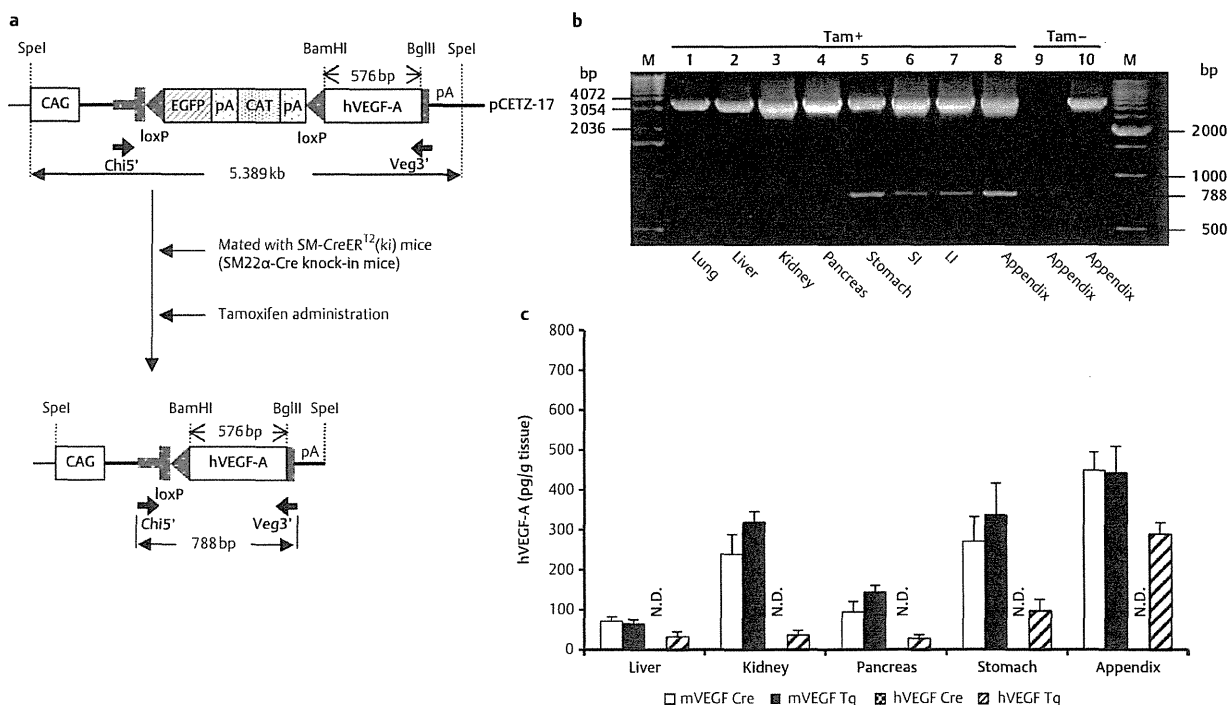


**Fig. 1** DNA constructs and Cre-mediated recombination. **a** Schema of the target plasmid (p-hVEGF-A<sup>fl</sup>) and its recombinant form. The *loxP* sites are shown as triangles. The small arrows (*Chi5'* and *Veg3'*) indicate the position and direction of the PCR primers. Tamoxifen was administered orally except for **b** (where administration was intraperitoneally). **b** Identification of the Cre-mediated DNA recombination product by PCR amplification of DNA isolated from SM-CreER<sup>T2</sup>/hVEGF (lanes 1–8), SM-CreER<sup>T2</sup>(ki) (lane 9), and hVEGF<sup>fl</sup> (lane 10) mice. The 788-bp fragment represents the recombinant DNA. M: size marker. Tam: tamoxifen. SI: small intestine. LI: large intestine. **c** Mouse and human VEGF-A protein expression in liver, kidney, pancreas, stomach and appendix vermiformis homogenate from SM-CreER<sup>T2</sup>/hVEGF (Tg) (*n*=6) and SM-CreER<sup>T2</sup>(ki) (Cre) (*n*=6) mice. N.D. = not detected.

(lane 9), and hVEGF<sup>fl</sup> (lane 10) mice. The 788-bp fragment represents the recombinant DNA. M: size marker. Tam: tamoxifen. SI: small intestine. LI: large intestine. **c** Mouse and human VEGF-A protein expression in liver, kidney, pancreas, stomach and appendix vermiformis homogenate from SM-CreER<sup>T2</sup>/hVEGF (Tg) (*n*=6) and SM-CreER<sup>T2</sup>(ki) (Cre) (*n*=6) mice. N.D. = not detected.

### VEGF-A expression analysis

To measure VEGF-A expression levels, liver, kidney, pancreas, stomach, and appendix ( $n=6$ ) were lysed in RIPA lysis buffer (Santa Cruz Biotechnology, Santa Cruz, CA, USA) supplemented with protease inhibitors (Halt Protease Inhibitor Cocktail; Pierce Biotechnology, Rockford, IL, USA). Tissues were then sonicated on ice, and centrifuged at  $10000\times g$  for 10 min at  $4^{\circ}\text{C}$ . Mouse and human VEGF-A concentrations in the supernatant was measured using a mouse or human VEGF ELISA kit (R&D Systems, Minneapolis, MN, USA), respectively.

### Immunohistochemistry

Tissue samples were fixed in 10% phosphate-buffered formalin for 24h at room temperature followed by paraffin embedding and examined by immunohistochemistry. Consecutive sections were incubated with rabbit anti-insulin (Cell Signaling Technology, Beverly, MA, USA; 1:200 dilution) followed by horseradish peroxidase-conjugated secondary antibody (Nichirei Bioscience, Tokyo, Japan). Staining was visualized with 3, 3'-diaminobenzidine (DAB) (DAKO, Carpinteria, CA, USA). Immunofluorescence was performed with chicken anti-insulin (Abcam, Cambridge, MA, USA; dilution 1:50), rabbit anti-glucagon (Cell Signaling Technology; 1:50), rabbit anti-somatostatin (ImmunoStar, Hudson, WI, USA; 1:400), or mouse anti-proliferating cell nuclear antigen (PCNA) (Cell Signaling Technology; 1:100) and subsequently incubated with fluorescently labeled secondary antibodies (Alexa Fluor 594, 488; Invitrogen, Carlsbad, CA, USA). The sections were examined under an ApoTome microscope (Carl Zeiss Inc., Oberkochen, Germany), and photographed with a charge-coupled device digital camera. Microscopic views were captured as digitized pictures using Axiovision software (Carl Zeiss Inc.). The area containing IPCs was analyzed using Image J 1.40 software (National Institute of Health, Bethesda, MD, USA). IPC clusters from 3–5 sections, obtained every  $300\mu\text{m}$  per pancreatic sample, were evaluated. The number of IPC clusters was counted and compared with that of control SM-CreER<sup>T2</sup>(ki) mice.

### Quantitative RT-PCR

Total RNA from tissues other than the pancreas was isolated with an RNAqueous Kit (Ambion, Austin, TX, USA). RNA extraction from pancreatic tissue was performed as described previously [9]. Briefly, pancreatic RNA samples were immediately frozen in liquid nitrogen and treated with RNAlater-ICE (Ambion). Total RNA was then isolated with an RNeasy Mini Kit (Qiagen, Valencia, CA, USA). For real-time quantitative RT-PCR (qRT-PCR), cDNA was reverse transcribed and amplified using TaqMan Gene Expression master mix on an ABI Prism 7300 (Applied Biosystems, Foster City, CA, USA). Expression levels of *Ins1* (Mm01259683\_g1), *Ins2* (Mm00731595\_g1), *Ngn3* (Mm00437606\_s1), *Pdx1* (Mm00435565\_m1), *Nkx6-1* (Mm00454962\_m1), and *Mafa* (Mm00845206\_s1) were normalized to *Gapdh* (Mm9999915\_g1) expression.

### Type I diabetes mice induced by streptozotocin

Mice were fasted for 8 h before inducing diabetes by STZ (Sigma, St. Louis, MO, USA) injection. STZ dissolved in saline on ice was administered intraperitoneally at a dose of 50 mg/kg body weight/day for 5 consecutive days. Mice not exhibiting diabetic symptoms received up to 3 additional 50 mg/kg of STZ doses, until fasting blood glucose levels of more than 300 mg/dL were reached.

### Statistical analysis

Results are presented as mean  $\pm$  SEM. Statistical analyses were performed using unpaired Student's *t*-test. Values of  $p < 0.05$  were considered statistically significant.

## Results

### Generation of transgenic mice with SMC-specific hVEGF-A expression

We generated mice overexpressing hVEGF-A in SMC by crossing *loxP*-flanked EGFP mice (hVEGF-A<sup>fl</sup>) with mice expressing Cre under the control of an SMC-specific promoter responding to tamoxifen (SM-CreER<sup>T2</sup>(ki)) ( $\odot$  Fig. 1a). Before recombination, the *loxP*-flanked EGFP/CAT hybrid sequence was expressed under control of the CAG promoter, while the *VEGFA* gene was silent [10]. All experiments were performed under tamoxifen administration and Cre-mediated recombination resulting in the deletion of the EGFP/CAT sequence and subsequent expression of *VEGFA*, resulting in SM-CreER<sup>T2</sup>/hVEGF transgenic mice. The presence of a 788-bp PCR product from SM-CreER<sup>T2</sup>/hVEGF mice confirmed successful recombination ( $\odot$  Fig. 1a, b). The transgene recombination was predominantly observed in visceral smooth muscle cells (SMCs), such as the gastrointestinal tract ( $\odot$  Fig. 1b).

Next, we examined hVEGF-A and mouse VEGF-A (mVEGF-A) protein levels in SM-CreER<sup>T2</sup>/hVEGF mice. hVEGF-A was detected dominantly in the stomach and the appendix of SM-CreER<sup>T2</sup>/hVEGF mice ( $97.9 \pm 72.5$  or  $290.5 \pm 74.3$  pg/mg tissue, respectively;  $\odot$  Fig. 1c). Expression of hVEGF-A in SM-CreER<sup>T2</sup>/hVEGF mice was moderate and hVEGF-A levels were less than mVEGF-A. hVEGF-A was not detected in the appendix of tamoxifen-treated SM-CreER<sup>T2</sup>(ki) mice, suggesting there was no cross-reactivity between hVEGF and mVEGF by ELISA assay. SM-CreER<sup>T2</sup>/hVEGF mice appeared normal and had normal body weights and life spans. The proportions of SM-CreER<sup>T2</sup>/hVEGF, SM-CreER<sup>T2</sup>(ki), hVEGF-A<sup>fl</sup>, and wild-type mice were in accordance with Mendelian ratios, at 26.2, 25.4, 20.7 and 27.7%, respectively.

### Small clusters of insulin producing cells increased in SM-CreER<sup>T2</sup>/hVEGF mice

Immunohistochemical examination was performed to determine the effect of enhanced SMC hVEGF-A expression on the pancreas. Morphologically distinct changes were not observed in pancreatic islets or exocrine tissues of tamoxifen-treated SM-CreER<sup>T2</sup>/hVEGF mice, compared with tamoxifen-treated SM-CreER<sup>T2</sup>(ki) mice. We did observe a number of small IPC clusters, in addition to pancreatic islets, in SM-CreER<sup>T2</sup>/hVEGF mice ( $\odot$  Fig. 2a). These IPCs were found as individual cells or as small clusters ( $\odot$  Fig. 2b). The number of small IPC clusters ( $100\text{--}215\mu\text{m}^2$ ) in SM-CreER<sup>T2</sup>/hVEGF mice increased significantly compared with SM-CreER<sup>T2</sup>(ki) mice (473 out of 1992 clusters IPCs in SM-CreER<sup>T2</sup>/hVEGF mice,  $n=5$  vs. 199 out of 976 in SM-CreER<sup>T2</sup>(ki) mice,  $n=3$ ,  $p < 0.05$ ) ( $\odot$  Fig. 2c). The proportion of IPC area, including small clusters of IPCs and islets, relative to exocrine area, was similar between SM-CreER<sup>T2</sup>/hVEGF and SM-CreER<sup>T2</sup>(ki) mice ( $\odot$  Fig. 2d). In addition, the number of pancreatic duct IPCs relative to those that were exocrine based was similar ( $\odot$  Fig. 2e). Double staining for glucagon or somatostatin and insulin was used to determine whether small IPC clusters consisted of only IPCs, or contained several types of endocrine

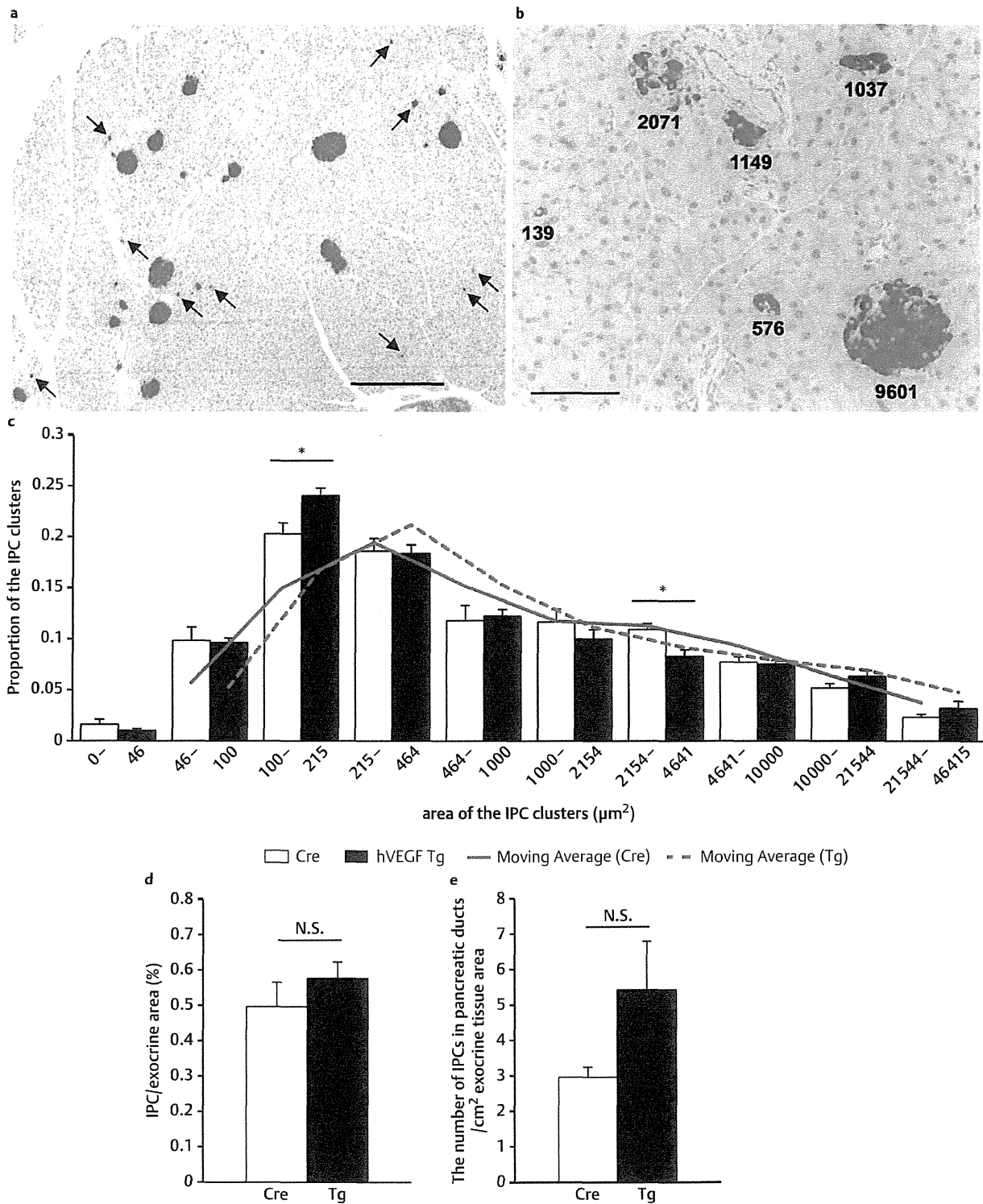


**Fig. 2** Small IPC clusters increased in SM-CreER<sup>T2</sup>/hVEGF mice, 4 weeks after hVEGF-A induction. **a** Immunohistochemistry of IPCs (brown) at 12 weeks of age; arrowheads: small IPC clusters. The scale bar indicates 500  $\mu\text{m}$ . **b** The area of each IPC ( $\mu\text{m}^2$ ). The scale bar indicates 100  $\mu\text{m}$ . **c** Proportion of IPC clusters according to size in 12-week-old mice. **d** IPC area over total exocrine area. **e** The number of IPCs in pancreatic ducts divided by total exocrine area ( $\text{cm}^2$ ). White bars: SM-CreER<sup>T2</sup>(ki) (Cre) mice (976 IPC clusters in total,  $n=3$ ); black bars: SM-CreER<sup>T2</sup>/hVEGF (Tg) mice (1992 IPC clusters in total,  $n=5$ ); Data represent mean  $\pm$  SEM. \*  $p < 0.05$ .

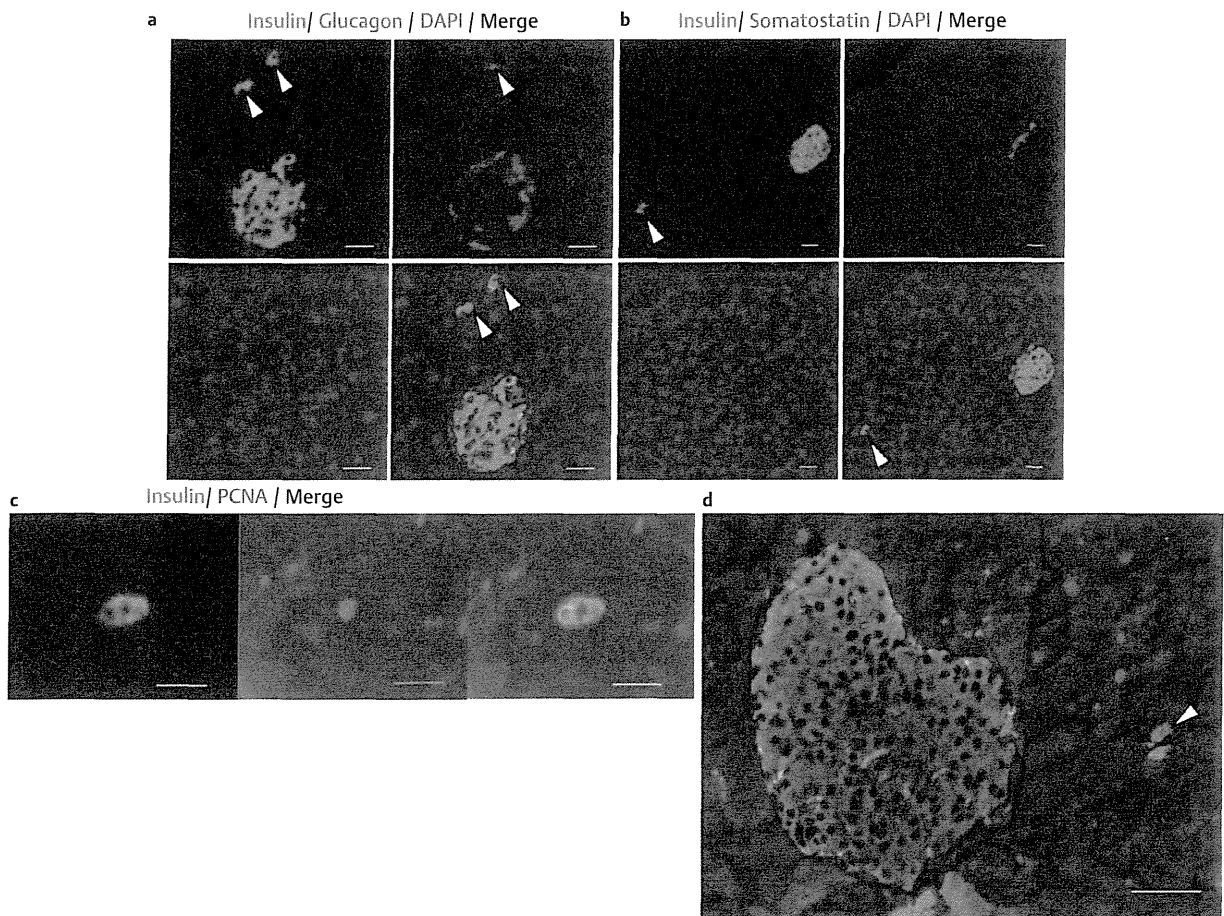


**Fig. 3** Immunofluorescence for insulin (red; a–d), glucagon (green; a), somatostatin (green; b) and 4',6-diamidino-2-phenylindole (DAPI) (blue; a and b) and PCNA (green; c and d) in SM-CreER<sup>T2</sup>/hVEGF mice. Arrowheads: individual IPCs or small IPC clusters. The scale bars indicate 100 μm (a and b), 20 μm c and 50 μm d.

**Table 1** Number of PCNA positive cells in SM-CreER<sup>T2</sup> (ki) (Cre) mice and SM-CreER<sup>T2</sup>/hVEGF (Tg) mice. The area of single IPCs or small IPC clusters was less than 215 μm<sup>2</sup>. Pancreatic sections were obtained every 300 μm.

	number of mice	number of sections	PCNA positive cells	single/small clusters of IPCs
SM22α-Cre	3	15	0	380
hVEGF Tg	5	28	2	770

cells, as is usually observed in pancreatic islets. Immunofluorescence revealed that most small clusters contained only IPCs, with very few containing glucagon-producing cells (○ Fig. 3a). Somatostatin-producing cells attached to the small clusters were not observed (○ Fig. 3b). Insulin and PCNA staining was then used to investigate the proliferative capacity of small IPC clusters. 2 individual IPCs were PCNA positive in SM-CreER<sup>T2</sup>/hVEGF mice out of 720 small IPC clusters (n=5, 28 sections). No PCNA positive cells were observed in SM-CreER<sup>T2</sup> (ki) mice out of 380 small IPC clusters (n=3, 15 sections) (○ Fig. 3c, d and ○ Table 1).

Although regeneration of the β-cell mass in adult mice is reportedly due to replication of existing differentiated β-cells rather than progenitor cell differentiation, adult pancreatic stem or progenitor cells residing in pancreatic ducts, islets, or bone mar-

row [11–15]. To investigate the origin of IPC clusters, qRT-PCR analysis was performed for *Ins1*, *Ins2*, *Nkx6-1*, *Pdx1*, *Ngn3*, and *Mafa*, key molecules in β-cell differentiation [16–18]. Our qRT-PCR analysis showed that *Ngn3* and *Mafa* gene expression increased approximately 1.5 fold in SM-CreER<sup>T2</sup>/hVEGF relative to SM-CreER<sup>T2</sup> (ki) mice, although this was not statistically significant. The expression of other genes was comparable in SM-CreER<sup>T2</sup>/hVEGF and SM-CreER<sup>T2</sup> (ki) mice (○ Fig. 4).

#### Effects of non-β cell-derived VEGF-A in STZ-induced diabetic mice

We next investigated the long-term effects of non-β cell-derived VEGF-A over expression in STZ-induced diabetic mice [19] (○ Fig. 5a). We administered STZ (50 mg/kg body weight/day) to mice for 5 consecutive days until the blood glucose level exceeded 300 mg/dL. If blood glucose levels did not reach 300 mg/dL, an additional 50 mg/kg dose was administered (3 times at most). The total quantity of additional STZ between SM-CreER<sup>T2</sup>/hVEGF and SM-CreER<sup>T2</sup> (ki) mice was not statistically significant, with fasting blood glucose levels in SM-CreER<sup>T2</sup>/hVEGF mice decreasing 3 weeks following hVEGF-A induction. However, a statistically significant improvement in fasting blood glucose, relative to diabetic SM-CreER<sup>T2</sup> (ki) mice, was observed at only one point in the 12 weeks following STZ administration

■ Proof copy for correction only. All forms of publication, duplication or distribution prohibited under copyright law. ■

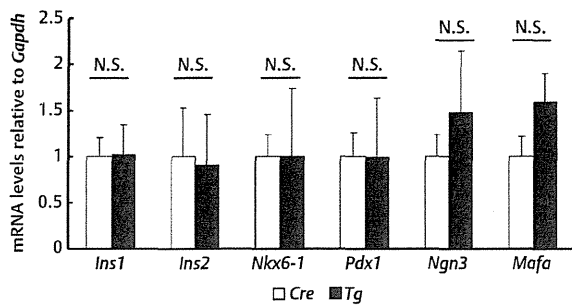


**Fig. 4** Real-time RT-PCR quantification of pancreatic gene expression. Pancreas was removed at 12 weeks of age, 4 weeks after hVEGF-A induction. Results are normalized to *Gapdh* expression. White bars: SM-CreER<sup>T2</sup> (ki) (n=5); black bars: SM-CreER<sup>T2</sup>/hVEGF (n=6); N.S.: not significant.

(○ Fig. 5a-d). Similarly, STZ-induced diabetic SM-CreER<sup>T2</sup>/hVEGF mice tended to weigh more than that SM-CreER<sup>T2</sup> (ki) mice, although this was not statistically significant (○ Fig. 5e).

## Discussion

Inducing endogenous  $\beta$ -cell regeneration is an attractive approach to reversing damage caused by type 1 and type 2 diabetes. Recent investigations have revealed that cells in the adult pancreas exhibit more plasticity than previously recognized [20]. Ogiwara et al. and Zhou et al. recently reported on the *in vivo* reprogramming of adult pancreatic exocrine cells to  $\beta$ -cells, without reversion to a pluripotent stem cell, by inducing 3 transcription factors (*Pdx1*, *Ngn3* and *Mafa*) [21,22]. Inada et al. demonstrated that pancreatic ductal cells act as progenitors that give rise to both new islets and normal acini after birth or injury

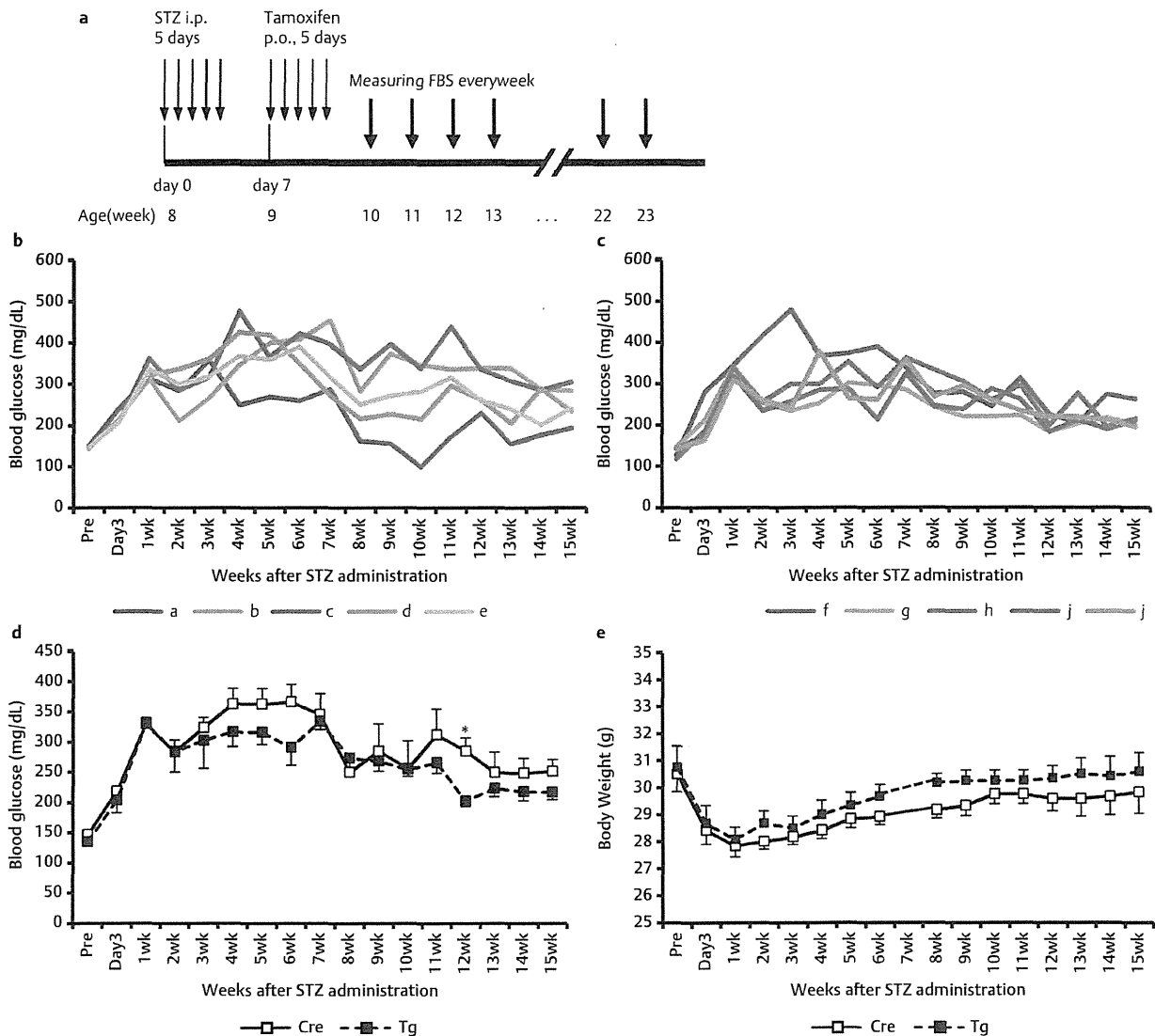


**Fig. 5** Effects of non- $\beta$  cell-derived VEGF-A in STZ-induced diabetic mice. **a** Time schedule for drug administration and fasting blood glucose measurements; i.p., intraperitoneally; p.o., per oral. **b, c** Fasting blood glucose levels before and after STZ administration in SM-CreER<sup>T2</sup>(ki) (Cre). (**b**, n=5, a-e) and SM-CreER<sup>T2</sup>/hVEGF (Tg) mice (**c**, n=5, f-j). **d** Statistical analysis of fasting blood glucose level from ○ Fig. 3b, c. Results are expressed as mean  $\pm$  SEM. \*  $p < 0.05$  **e** Body weight before and after STZ administration in SM-CreER<sup>T2</sup> (ki) (Cre) and SM-CreER<sup>T2</sup>/hVEGF (Tg) mice. Results are expressed as mean  $\pm$  SEM.

■ Proof copy for correction only. All forms of publication, duplication or distribution prohibited under copyright law. ■

[23]. In addition, Talchai et al. demonstrated that  $\beta$ -cells under hyperglycemic conditions dedifferentiate and revert to progenitor-like cells in Foxo1 deficient mice [24]. This suggests that pancreatic cells, both exocrine and endocrine, can change their properties to adapt to their environment.

In this study, we generated mice expressing hVEGF-A in SMCs using the Cre-LoxP recombination system. VEGF-A deficient mice die embryonically, as do heterozygous VEGF-A mice. In contrast, mice overexpressing VEGF-A<sub>121</sub> or VEGF-A<sub>189</sub> suffer from hyper-permeability and/or hypervascularization, whereas mice overexpressing VEGF-A<sub>165</sub> are born relatively healthy [25]. Interestingly, our mice displayed moderate hVEGF-A<sub>165</sub> expression in SMCs, and SM-CreER<sup>T2</sup>/hVEGF mice showed no obvious changes in their pancreatic tissues.

Recent reports revealed that a hyperglycemic or hyperosmolar state induces VEGF-A secretion in vascular smooth muscle cells [26,27]. As VEGF-A<sub>165</sub> has a heparin-binding region, some of it likely binds to heparin on the cell surface or to heparin sulfate proteoglycan in the extracellular matrix, and topically serves the angiogenic effects where it is released, while VEGF<sub>165</sub> may be released to the blood stream or incorporated by platelets. Thus, it might be active at a place distant from the site of secretion [28–30].

We showed that upregulation of VEGF-A in SMCs significantly increases small IPC clusters in the pancreas and decreases the proportion of middle-sized islets (© Fig. 2c). *Transgelin/SM22 $\alpha$*  is expressed in both vascular and visceral SMCs. The phenomenon observed above is partly due to increased VEGF-A derived from pancreatic vascular SMCs, but in large part the phenomenon is likely due to increased VEGF-A from visceral SMCs of the alimentary tract, as suggested by RT-PCR and VEGF-A ELISA results (© Fig. 1b, c). Although most small IPC clusters observed in SM-CreER<sup>T2</sup>/hVEGF mice were not accompanied by  $\alpha$  and/or  $\delta$  cells, some small IPC clusters were attached to a single or a few  $\alpha$  cells (© Fig. 3a, b), of which 2 individual IPCs were PCNA positive (© Fig. 3c, d). This suggests that small IPC clusters in SM-CreER<sup>T2</sup>/hVEGF mice have ability to proliferate in a similar developmental process and were forming functional islets [31].

We found some IPCs in the pancreatic ducts may be candidate  $\beta$ -cell progenitors [23], but the number of these cells in SM-CreER<sup>T2</sup>/hVEGF mice was similar to that of SM-CreER<sup>T2</sup>(ki) mice (© Fig. 2e). Although additional studies are required to determine the major pathways involved in IPC regeneration, it may be that the relatively high expression of *Ngn3* and *Mafa* in SM-CreER<sup>T2</sup>/hVEGF mice induced pancreatic endocrine progenitor cells and/or exocrine cells to regenerate IPCs [22]. The factors from fetal pancreatic cells that induce differentiation into endocrine cells are not fully known. Nor is it known whether endocrine progenitors in adult mice undergo the same process as seen in fetal  $\beta$ -cell development. In our study, VEGF-A increased the population of small IPC clusters. This might be caused either by a direct effect of non- $\beta$  cell-derived VEGF-A or by the subsequent accumulation of endothelial/SMC-mediated signals to the pancreas. Recently, both protective and harmful effects to glucose metabolism by time-dependent VEGF-A over expression in islets have been reported [32]. However, non- $\beta$  cell-derived VEGF-A in STZ-induced diabetic mice did not exhibit toxic effects to glycemic control, and may in fact improve the diabetic conditions in these mice (© Fig. 5a–e). Thus, VEGF-A expressed from SMCs is closely associated with glucose metabolism and may have an important adaptive role in protecting against hyperglycemia in vivo.

**Disclosure of conflict of interest:** The authors do not declare any conflict of interests.

#### Affiliations

- <sup>1</sup> Department of Laboratory and Vascular Medicine, Graduate School of Medical and Dental Sciences, Kagoshima University, Sakuragaoka, Kagoshima, Japan
- <sup>2</sup> Department of Ophthalmology, Kagoshima University Graduate School of Medical and Dental Sciences, Sakuragaoka, Kagoshima, Japan
- <sup>3</sup> Department of Veterinary Experimental Animal Science, Faculty of Agriculture, Kagoshima University, Korimoto, Kagoshima, Japan
- <sup>4</sup> Systems Biology in Thromboregulation, Kagoshima University Graduate School of Medical and Dental Sciences, Sakuragaoka, Kagoshima, Japan
- <sup>5</sup> Interfakultäres Institut für Biochemie, University of Tübingen, Tübingen, Germany
- <sup>6</sup> Laboratory of Functional Foods, Department of Biomedical Engineering Osaka Institute of Technology, Osaka, Japan

#### References

- 1 Lammert E, Cleaver O, Melton D. Induction of pancreatic differentiation by signals from blood vessels. *Science* 2001; 294: 564–567
- 2 Lammert E, Gu G, McLaughlin M et al. Role of VEGF-A in vascularization of pancreatic islets. *Curr Biol* 2003; 13: 1070–1074
- 3 Brissava M, Shostak A, Shiota M et al. Pancreatic islet production of vascular endothelial growth factor-A is essential for islet vascularization, revascularization, and function. *Diabetes* 2006; 55: 2974–2985
- 4 Kuhbandner S, Brummer S, Metzger D et al. Temporally controlled somatic mutagenesis in smooth muscle. *Genesis* 2000; 28: 15–22
- 5 Feil S, Hofmann F, Feil R. SM22alpha modulates vascular smooth muscle cell phenotype during atherosclerosis. *Circ Res* 2004; 94: 863–865
- 6 Sato M, Yasuoka Y, Kodama H et al. New approach to cell lineage analysis in mammals using the Cre-loxP system. *Mol Reprod Dev* 2000; 56: 34–44
- 7 Shrestha B, Hashiguchi T, Ito T et al. B cell-derived vascular endothelial growth factor A promotes lymphangiogenesis and high endothelial venule expansion in lymph nodes. *J Immunol* 2010; 184: 4819–4826
- 8 Hem A, Smith AJ, Solberg P. Saphenous vein puncture for blood sampling of the mouse, rat, hamster, gerbil, guinea pig, ferret and mink. *Lab Anim* 1998; 32: 364–368
- 9 Kiba T, Kintaka Y, Nakada E et al. High-quality RNA extraction from rat pancreas for microarray analysis. *Pancreas* 2007; 35: 98–100
- 10 Niwa H, Yamamura K, Miyazaki J. Efficient selection for high-expression transfectants with a novel eukaryotic vector. *Gene* 1991; 108: 193–199
- 11 Bonner-Weir S, Baxter LA, Schupp GT et al. A second pathway for regeneration of adult exocrine and endocrine pancreas. A possible recapitulation of embryonic development. *Diabetes* 1993; 42: 1715–1720
- 12 Dor Y, Brown J, Martinez OI et al. Adult pancreatic beta-cells are formed by self-duplication rather than stem-cell differentiation. *Nature* 2004; 429: 41–46
- 13 Xu X, D'Hoker J, Stange G et al. Beta cells can be generated from endogenous progenitors in injured adult mouse pancreas. *Cell* 2008; 132: 197–207
- 14 Zajicek G, Arber N, Schwartz-Arad D et al. Streaming pancreas: islet cell kinetics. *Diabetes Res* 1990; 13: 121–125
- 15 Zulewski H, Abraham EJ, Gerlach MJ et al. Multipotential nestin-positive stem cells isolated from adult pancreatic islets differentiate ex vivo into pancreatic endocrine, exocrine, and hepatic phenotypes. *Diabetes* 2001; 50: 521–533
- 16 Best M, Carroll M, Hanley NA et al. Embryonic stem cells to beta-cells by understanding pancreas development. *Mol Cell Endocrinol* 2008; 288: 86–94
- 17 Murtaugh LC. Pancreas and beta-cell development: from the actual to the possible. *Development* 2007; 134: 427–438
- 18 Zaret KS, Grompe M. Generation and regeneration of cells of the liver and pancreas. *Science* 2008; 322: 1490–1494
- 19 Lenzen S. The mechanisms of alloxan- and streptozotocin-induced diabetes. *Diabetologia* 2008; 51: 216–226
- 20 Demeterco C, Hao E, Lee SH et al. Adult human beta-cell neogenesis? *Diabetes Obes Metab* 2009; 11 (Suppl 4): 46–53
- 21 Ogihara T, Fujitani Y, Uchida T et al. Combined expression of transcription factors induces AR42J-B13 cells to differentiate into insulin-producing cells. *Endocr J* 2008; 55: 691–698

- 22 Zhou Q, Brown J, Kanarek A *et al.* In vivo reprogramming of adult pancreatic exocrine cells to beta-cells. *Nature* 2008; 455: 627–632
- 23 Inada A, Nienaber C, Katsuta H *et al.* Carbonic anhydrase II-positive pancreatic cells are progenitors for both endocrine and exocrine pancreas after birth. *Proc Natl Acad Sci USA* 2008; 105: 19915–19919
- 24 Talchai C, Lin HV, Kitamura T *et al.* Genetic and biochemical pathways of beta-cell failure in type 2 diabetes. *Diabetes Obes Metab* 2009; 11 (Suppl 4): 38–45
- 25 Olsson AK, Dimberg A, Kreuger J *et al.* VEGF receptor signalling – in control of vascular function. *Nat Rev Mol Cell Biol* 2006; 7: 359–371
- 26 Doronzo G, Viretto M, Russo I *et al.* Effects of high glucose on vascular endothelial growth factor synthesis and secretion in aortic vascular smooth muscle cells from obese and lean Zucker rats. *Int J Mol Sci* 2012; 13: 9478–9488
- 27 Oberg-Welsh C, Sandler S, Andersson A *et al.* Effects of vascular endothelial growth factor on pancreatic duct cell replication and the insulin production of fetal islet-like cell clusters in vitro. *Mol Cell Endocrinol* 1997; 126: 125–132
- 28 Klement GL, Yip TT, Cassiola F *et al.* Platelets actively sequester angiogenesis regulators. *Blood* 2009; 113: 2835–2842
- 29 Park JE, Keller GA, Ferrara N. The vascular endothelial growth factor (VEGF) isoforms: differential deposition into the subepithelial extracellular matrix and bioactivity of extracellular matrix-bound VEGF. *Mol Biol Cell* 1993; 4: 1317–1326
- 30 Robinson CJ, Stringer SE. The splice variants of vascular endothelial growth factor (VEGF) and their receptors. *J Cell Sci* 2001; 114: 853–865
- 31 Jorgensen MC, Ahnfelt-Ronne J, Hald J *et al.* An illustrated review of early pancreas development in the mouse. *Endocr Rev* 2007; 28: 685–705
- 32 De Leu N, Heremans Y, Coppens V *et al.* Short-term overexpression of VEGF-A in mouse beta cells indirectly stimulates their proliferation and protects against diabetes. *Diabetologia* 2013



## メタボリックストレスと自然炎症

伊藤 隆史

Ito Takashi

鹿児島大学大学院医歯学総合研究科システム血栓制御学（メディポリス連携医学）講座

### Points

- ①インフラマソームの異常活性化は、多くの自己炎症疾患の病態の中核をなしている。
- ②高尿酸、高血糖、高コレステロール、高中性脂肪などのメタボリックストレスは、インフラマソームを活性化して、自然炎症を引き起こす。
- ③メタボリックストレスによって、HMGB1 やヒストンなどの核内蛋白質は細胞外へと放出され、炎症や血栓傾向を引き起こす。

### Key Words

- ▼自己炎症疾患
- ▼インフラマソーム
- ▼インターロイキン 1 $\beta$  (IL-1 $\beta$ )
- ▼HMGB1
- ▼ヒストン

### はじめに ～自己炎症疾患の原因～

自己炎症疾患 (autoinflammatory diseases) は、マクロファージ、単球、好中球などの自然免疫細胞が明らかな誘因なく異常に活性化する疾患群で、獲得免疫系の異常 (自己抗体や自己反応性リンパ球など) で引き起こされる自己免疫疾患 (autoimmune diseases) とは区別される。狭義には遺伝性周期性発熱症候群を指し、一般的な感染症では説明のつかない発熱のエピソードをくり返す。広義にはベーチェット病、クローン病、痛風なども自己炎症疾患と考えられている。病変の首座は皮膚、腹膜、胸膜、関節、眼、消化管などで、これらの部位で無菌性炎症をくり返すのが特徴である。1990 年代後半から 2000 年代にかけて、遺伝性周期性発熱症候群の原因

遺伝子がつぎつぎと同定され、その多くは、インフラマソームの異常活性化につながる変異であることが判明した<sup>1)</sup>。インフラマソームは炎症性サイトカインであるインターロイキン 1 $\beta$  (interleukin-1 $\beta$  : IL-1 $\beta$ ) を活性化して放出するための細胞内装置である (図①)。通常は感染や組織損傷の兆候を察知した際に活性化されるが、遺伝性周期性発熱症候群患者では、インフラマソームの構成因子や制御因子に変異があり、常時活性化されているか、活性化されやすい状態になっているため、明らかな誘因がないにもかかわらず IL-1 $\beta$  が活性化されて放出される。インフラマソーム-IL-1 $\beta$  経路の異常活性化は、多くの自己炎症疾患の病態の中核をなしているのである。

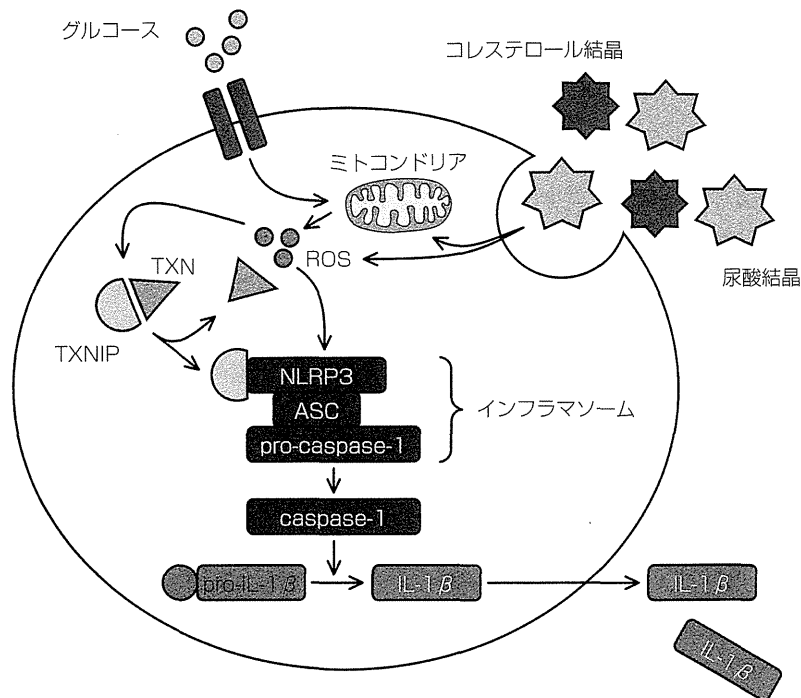


図1 インフラマソームはIL-1βを活性化するための細胞内装置である

遺伝性周期性発熱症候群では、インフラマソームの構成因子や制御因子に変異があり、明らかな誘因がないにもかかわらずIL-1βが活性化されて放出される。高尿酸、高血糖、高コレステロールなどの代謝的ストレスは、ミトコンドリアの機能不全や傷害を引き起こし、これによってROSの産生、漏出が増加する。ROSが増加すると、TXNIPが本来の結合相手であるTXNから離れ、インフラマソームに結合してこれを活性化する。

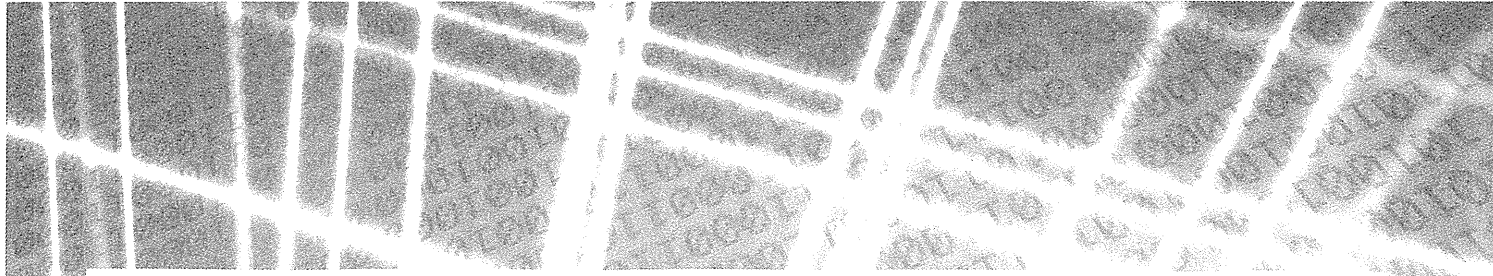
ROS: reactive oxygen species (活性酸素種), TXN: thioredoxin (チオレドキシン), TXNIP: thioredoxin interacting protein (チオレドキシン結合蛋白質), NLRP3: NOD-like receptor family, pyrin domain containing 3, ASC: apoptosis-associated speck-like protein containing a CARD

## 1. 代謝的ストレスとインフラマソーム

痛風、糖尿病、動脈硬化症などの生活習慣病も、広義の自己炎症疾患としてとらえる動きがある。これらの疾患においても、インフラマソーム-IL-1β経路の活性化とそれに伴う無菌性炎症が病態に深くかかわっている可能性が示唆されているからである<sup>2)</sup>。痛風は尿酸塩結晶による結晶誘発性関節炎である。尿酸の体液中での飽和濃度は、血清尿酸値で約7mg/dLであり、これを超えると容易に結晶化して沈着する。この尿酸塩結晶の沈着が痛風を引き起こすわけだが、近年、その機序として、

尿酸塩結晶が単球・マクロファージのインフラマソームを活性化し、IL-1β放出を誘導していることが明らかになった<sup>2)</sup>。IL-1受容体拮抗薬は、マウスにおいて尿酸塩結晶誘発関節炎による炎症と痛みを軽減し、ヒトにおいても治療抵抗性痛風患者の症状を軽減する可能性が報告されている<sup>2)</sup>。また、痛風発作や遺伝性周期性発熱症候群の寛解を目的として、臨床の現場でしばしば用いられるコルヒチンは、作用機序として、インフラマソームの活性化を抑制していることも明らかになった<sup>2)</sup>。

2型糖尿病でもインフラマソーム-IL-1β経路の関与が注目されている。高血糖が持続すると、膵β細胞のインスリン分泌能が低下するとともに、膵β細胞死が誘導さ



れる。この過程に IL-1 $\beta$  がかかわっていて、IL-1 受容体拮抗薬は、マウスおよびヒトにおいて膵 $\beta$ 細胞のインスリン分泌能を改善し、血糖コントロールを改善する。興味深いことに、IL-1 $\beta$  は少量 (pg/mL のオーダー) の場合には、膵 $\beta$ 細胞の増殖を誘導し、量が増えると (ng/mL のオーダー)、膵 $\beta$ 細胞死を誘導する。このことから、糖尿病の病態の初期に少量の IL-1 $\beta$  が分泌されることは、高血糖状態に対する適応反応である可能性が考えられ、この状態が遷延したり増悪したりすると、IL-1 $\beta$  はむしろ病態を悪化させる要因になりうると考えられる。糖尿病の際に IL-1 $\beta$  が分泌される機序としては、高血糖状態によって増加する活性酸素種 (reactive oxygen species : ROS) が関与していると考えられている。ROSが増加すると、チオレドキシシン結合蛋白質 (thioredoxin interacting protein : TXNIP) が本来の結合相手であるチオレドキシシン (TXN) から離れ、インフラマソームに結合してこれを活性化する<sup>3)</sup>。この ROS-TXNIP-インフラマソーム-IL-1 $\beta$  経路の活性化は、さまざまなメタボリックストレスに対する共通の応答系であると考えられ、痛風および糖尿病に共通の病態基盤となっている可能性が示唆される (図1)。

動脈硬化の進行にも IL-1 は重要な役割を果たしている。尿酸塩結晶がインフラマソーム-IL-1 $\beta$  経路を活性化して痛風の病態を悪化させるのと同様、高コレステロール環境下では、微細コレステロール結晶がインフラマソーム-IL-1 $\beta$  経路を活性化し、動脈硬化の初期病変としての血管炎症を引き起こす<sup>4)</sup>。動脈硬化の進行には、さらに、インフラマソーム非依存性の IL-1 $\alpha$  活性化経路も関係していて、この経路はオレイン酸などの脂肪酸によって活性化される<sup>5)</sup>。このように、高尿酸、高血糖、高コレステロール、高中性脂肪などのメタボリックストレス環境下では、細胞は IL-1 を分泌して適応しようとするが、これが関節、膵臓、血管などに自然炎症を引き起こし、生活習慣病の基盤を形成していると考えられる。

## 2. メタボリックストレスと HMGB1・ヒストン

メタボリックストレスはインフラマソームの活性化を介して IL-1 $\beta$  分泌を引き起こすほか、HMGB1 (high mobility group box 1) やヒストンなどの核内蛋白質の細胞外への放出も引き起こす。とくに、高脂肪食を摂取したり脂肪酸を負荷したりすると、HMGB1 やヒストンは細胞外に放出される<sup>6) 7)</sup>。ヒストンの細胞外への放出機序についてはほとんどわかっていないが、HMGB1 の細胞外への放出過程には、一部でインフラマソームが関与していることも報告されている<sup>8)</sup>。細胞外に放出されたヒストンは、血管内皮細胞を活性化して組織因子や接着因子の発現を増強するため、メタボリックストレス環境下での自然炎症や血栓傾向に関与している可能性が示唆される。これらの核内蛋白質が細胞外に放出されることも、本来はストレスに対する適応反応の一種だと考えられるが、その詳細は明らかになっていない。

## おわりに

インフラマソームのセンサー部分是一种のストレス感知装置になっていて、高尿酸、高血糖、高コレステロール、高中性脂肪などのメタボリックストレスを感知すると、アダプターを介してエフェクターを稼働させる。エフェクターが稼働すると、IL-1 $\beta$  や HMGB1 の放出という形で出力され、炎症が誘発される。インフラマソーム-IL-1 $\beta$  経路の活性化は、多くの自己炎症疾患の病態の中核をなしていると考えられていて、この経路をターゲットにした新規治療法の開発が進められている。

## 文献

- 1) Park H *et al* : Lighting the fires within : the cell biology of autoinflammatory diseases. *Nat Rev Immunol* 12 : 570-580, 2012
- 2) Schroder K *et al* : The NLRP3 inflammasome : a sensor for metabolic danger? *Science* 327 : 296-300, 2010

- 3) Zhou R *et al* : Thioredoxin-interacting protein links oxidative stress to inflammasome activation. *Nat Immunol* **11** : 136-140, 2010
- 4) Duewell P *et al* : NLRP3 inflammasomes are required for atherogenesis and activated by cholesterol crystals. *Nature* **464** : 1357-1361, 2010
- 5) Freigang S *et al* : Fatty acid-induced mitochondrial uncoupling elicits inflammasome-independent IL-1  $\alpha$  and sterile vascular inflammation in atherosclerosis. *Nat Immunol* **14** : 1045-1053, 2013
- 6) Li L *et al* : Nuclear factor high-mobility group box1 mediating the activation of Toll-like receptor 4 signaling in hepatocytes in the early stage of nonalcoholic fatty liver disease in mice. *Hepatology* **54** : 1620-1630, 2011
- 7) Shrestha C *et al* : Saturated fatty acid palmitate induces extracellular release of histone H3 : a possible mechanistic basis for high-fat diet-induced inflammation and thrombosis. *Biochem Biophys Res Commun* **437** : 573-578, 2013
- 8) Lu B *et al* : Regulation of HMGB1 release by inflammasomes. *Protein Cell* **4** : 163-167, 2013